CEPT

CEPT ECC
Electronic Communications Committee

ECC Report 321

Radio frequency test methods, tools and test results for wind turbines in relation to the Radio Astronomy Service

approved 2 October 2020

0 EXECUTIVE SUMMARY

The deployment of wind turbines in Europe is large and will become even larger in the future.

This Report is intended to be used as a source of information for those who will have the challenge to perform measurements for several reasons on wind turbines in relation to the radio astronomy service.

This Report is divided in annexes for which a number of individuals from administrations, scientific organisations and industry are responsible.

TABLE OF CONTENTS

LIST OF ABBREVIATIONS

Abbreviation	Explanation
BNetzA	Federal Network Agency
CEPT	European Conference of Postal and Telecommunications Administrations
CISPR	International Special Committee on Radio Interference
CRAF	Committee on Radio Astronomy Frequencies
DVB-T	Terrestrial Digital Video broadcasting
ECC	Electronic Communications Committee
EM	Electromagnetic
EMC	Electromagnetic Compatibility
EMI	Electromagnetic Interference
ITE	Information Technology Equipment
ITU	International Telecommunication Union
LIDAR	Light Detection and Ranging
LNA	Low Noise Amplifier
LOFAR	Low Frequency Array
MMN	Man Made Noise
MPIfR	Max Planck Institute for Radio Astronomy
PV	Photo Voltaic
QP	Quasi peak
RAS	Radio Astronomy Service
RCS	Radar Cross Section
RMS	Root Mean Square
RR	Radio Regulations
SRTM	(Space) Shuttle Radar Topography Mission
UHF	Ultra High Frequency
WT	Wind Turbine

1 INTRODUCTION

The deployment of wind turbines in Europe does not only bring geographical planning challenges but also challenges in terms of spectrum management.

ECC Report 260 [1] deals with the effects of wind turbines on fixed links. The present Report has the intention to provide information on the effects of wind turbines on the radio astronomy service and related measurements.

2 OVERVIEW OF MEASUREMENT METHODS AND RESULTS

2.1 MEASUREMENT SYSTEM FOR THE MEASUREMENT OF VERY LOW EMC LEVELS TO PROTECT THE RADIOASTRONOMY IN THE FREQUENCY RANGE 30-240 MHZ (LOFAR)

In the Netherlands, wind turbine parks are deployed at several locations including near sites used by the radio astronomy service. In order to specifically protect the LOFAR radio telescope, specific emission requirements for these wind turbines are defined based on the generic EMC limit: thus the allowed emissions are -50 dB for continuous operations and -35 dB below this limit for restricted operation for wind turbines near the telescope. The limit itself is defined as an e.i.r.p. emission with a power spectral density value of -180 dBm/Hz. These extremely low levels pose a challenge to measure specially since a calibrated measurement with traceable measurement uncertainty is needed. A method was developed within an expert group lead by the Radiocommunications agency in the Netherlands to measure these levels. The outline of the method, waiting for formal publication, is described in Annex 1.

2.1.1 A note about the topography of RAS stations

The following two figures show the difference in topography of Radio Telescope Effelsberg and Westerbork Synthesis Radio Telescope at the same height and distance scale. The figures are 50x50 km and generated with the pycraf tool as described in Annex 3 and [12], the white cross indicates the position of the telescopes. It is clear that assumptions and studies for this type of installation can only be performed for a national situation since topography may or may not provide additional mitigation against ground based interferers.

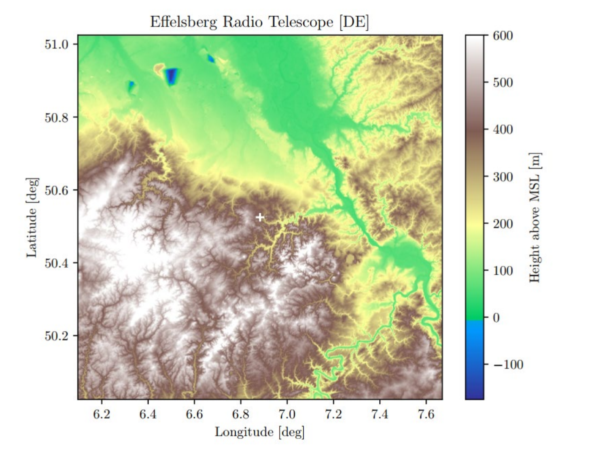

Figure 1: Topographic map Effelsberg

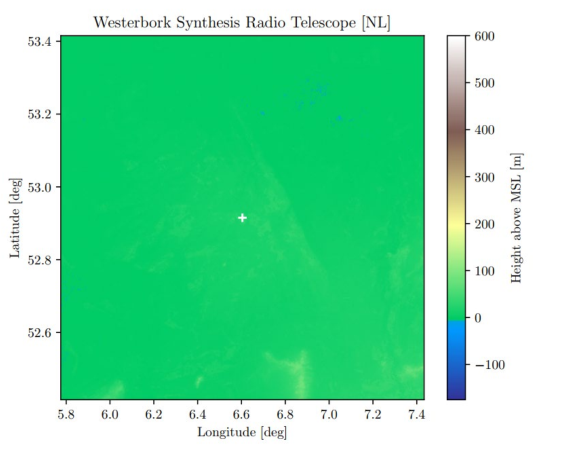

Figure 2: Topographic map Westerbork

2.2 MEASUREMENT RESULTS AND MEASUREMENT METHODS FOR THE PROTECTION OF THE RADIO ASTRONOMY SERVICE IN THE FREQUENCY RANGES AROUND 611 AND 1413 MHZ

During the years 2015 and 2016 the radio monitoring services of Munich and Constance of the Federal Network Agency, Germany, performed measurements of electromagnetic radiation at some types of modern three-bladed wind energy plants which are deployed on-shore in Germany. The towers are in pipe construction with hub-heights between 134 and 140 m. The rotor-diameters ranged from 80 to 130 m. The nominal powers were 2.3 MW, 2.4 MW and 3.3 MW.

The intention of the investigation was the protection of the Radio Telescope Effelsberg near Bonn against electromagnetic radiation from planned wind turbines in its geographical environment. Although the telescope is located in a valley providing a good shielding against EM radiation from nearby sources, the hub of wind turbines being 130 m above ground may have line-of-sight to the telescope even if it is installed several kilometres away. Due to its extreme receiver sensitivity, the radio telescope may be interfered even by very low power emissions.

Measuring the radiation from the hubs of wind turbines from the outside at close distances would require a mobile crane which is very expensive. The closest measurement distance on the ground is around 150 m away from the wind turbine. However, it turned out that the levels of emissions originating from the hubs of wind turbines in the UHF frequency ranges even at these distances are far below the general radio noise levels, and also below the noise floor of measurement receivers.

To be able to measure extremely weak signal levels requires:

- Measurement antennas with high directivity and gain;
- Very low noise preamplifier;
- Spectrum analyser or measurement receiver with highly stable noise level.

Knowledge of the signal characteristics in order to determine the optimum settings like bandwidth, detector and measurement time.

The characteristics of the wind turbine signals were determined by performing measurements directly at the possible emission sources (generators, regulators, transformers etc.) inside the hub of the wind turbines. It turned out that most of the emissions were broadband and/or noise-like, requiring a high measurement bandwidth.

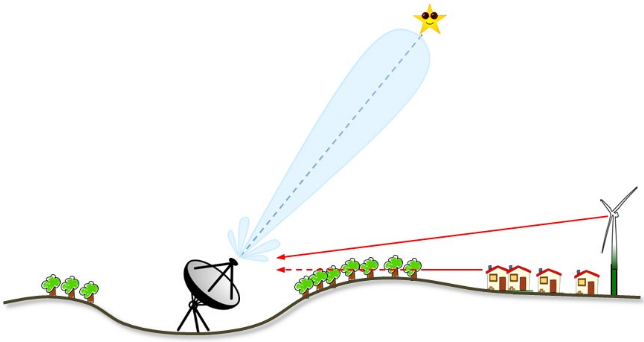

Figure 3: Interference scenario

To measure noise-like signals most accurately, the RMS levels as are averaged over a long-measurement time (e. g. 85 s) with a high measurement bandwidth (e. g. 10 MHz). Separation of the noise component from the wind turbine and the remaining radio noise was done by using directional measurement antennas.

From a ground position about 150 m away from the wind turbine, the total noise levels were measured in the direction of the wind turbine ("on-position") and in other directions away from the wind turbine ("off-positions").

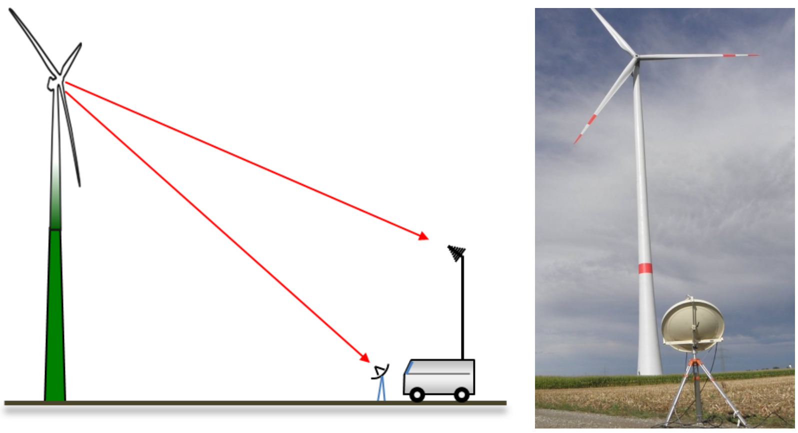

Figure 4: Measurement scenario

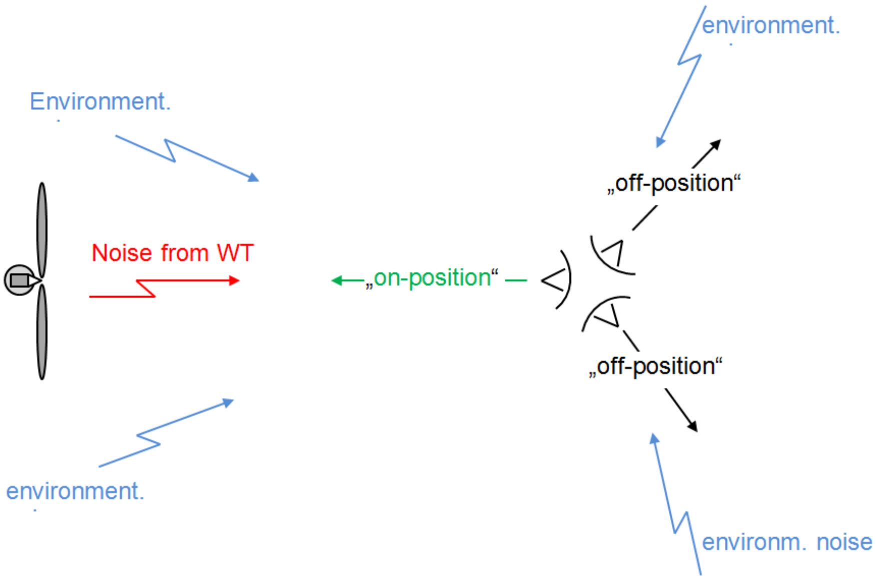

Figure 5: Measurement scenario

Subtracting both results (in linear units) reveals the noise component coming from the wind turbine. This principle works under the assumption that the environmental radio noise (atmospheric, galactic and man-made) is arriving equally from all directions and is not time dependent. The method also removes the receiver noise component which is constant in all measurements. The below figure shows the result for the frequency range 1411 MHz (blue = on-position, red = off-position). The difference between both positions, converted back into logarithmic values is about 0.14 dB.

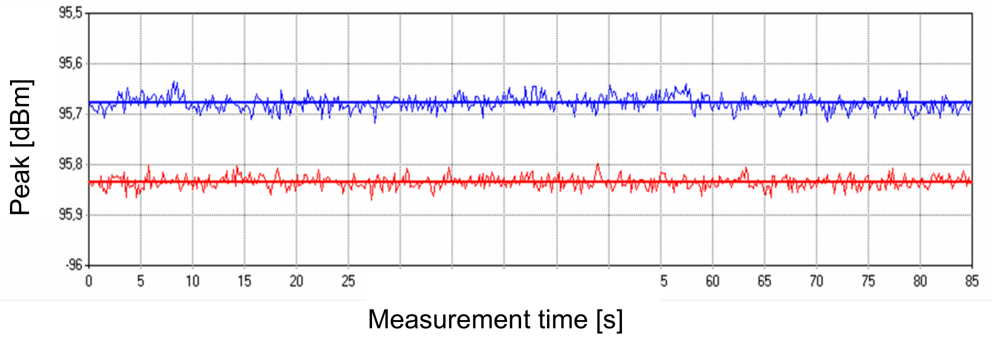

Figure 6: Measurement results for 1411 MHz (blue on / red off)

Received power in the on and off position and the resulting received wind turbine power (PWT) is as follows:

P_{off} = -95.84 dBm = 2.606E-10 mW;

P_{on} = -95.68 dBm = 2.704E-10 mW;

PWT = P_{on} – P_{off} = 0.098E-10 mW = -110 dBm.

From this received level, the emitted power of the wind turbine emission can be calculated using the antenna gain and the free-space loss calculated for the given measurement distance.

The maximum determined level of the radiated spectral power density from the wind turbines under test (PEMC) was -147 dB(W/Hz) in the frequency range 610 MHz and -150 dB(W/Hz) in the frequency range 1413 MHz.

According to Recommendation ITU-R RA.769-2 [15] the maximum acceptable interference spectrum-power-flux-density (pfd) is -253 dB(W/(Hz.m^2)) for the radio astronomy band near 611 MHz and -255 dB(W/(Hz.m^2)) for the radio astronomy band near 1413 MHz. Since the radio telescope is never pointed directly towards a wind turbine, interferences from all sources on the ground are received through side lobes of the antenna for which a gain of 0 dBi is assumed.

Using the equation:

$$L = PEMC - pdf - 10\log_{10}(\lambda^2/4\pi) \quad (1)$$

the required path loss between wind turbine and radio telescope L would be 130 dB for the radio-astronomy band near 611 MHz and 135 dB for the radio-astronomy band near 1413 MHz. Taking into account, the terrain and the propagation model of Recommendation ITU-R P.452, the resulting geographical protection distances around the Radio Telescope Effelsberg would be between 7 and 25 km for an assumed hub-height of 140 m.

Details of the measurements can be found in Annex 2.

2.3 A METHODOLOGY FOR RAS – WIND TURBINE COMPATIBILITY STUDIES

The document in reference [15] provided by CRAF provides only a very general outline of the compatibility considerations for wind turbines and RAS. Meanwhile more research has been done and published, including a publicly available Python software package that enables the user to carry out a fully-fledged compatibility calculation that includes terrain information. Annex 3 describes the findings and the software package. An example study for the German RAS station Effelsberg is also provided. This submission has been compiled by using extracts from the recent publication by B. Winkel & A. Jessner [4] and [5].

The methodology assumes that wind turbines emit a certain power level into the RAS bands (limited to the levels described in CISPR-11 [20], which represents a worst-case scenario). It then applies the path propagation loss according to Recommendation ITU-R P.452-16 [3] that includes line of sight loss, diffraction at real terrain, tropospheric scatter and anomalous propagation. Finally, the resulting received powers are compared to the RAS threshold levels specified in to Recommendation ITU-R RA.769-2 [15], which allows to calculate the link margins, which help to define necessary protection zones, see for example Figure 7.

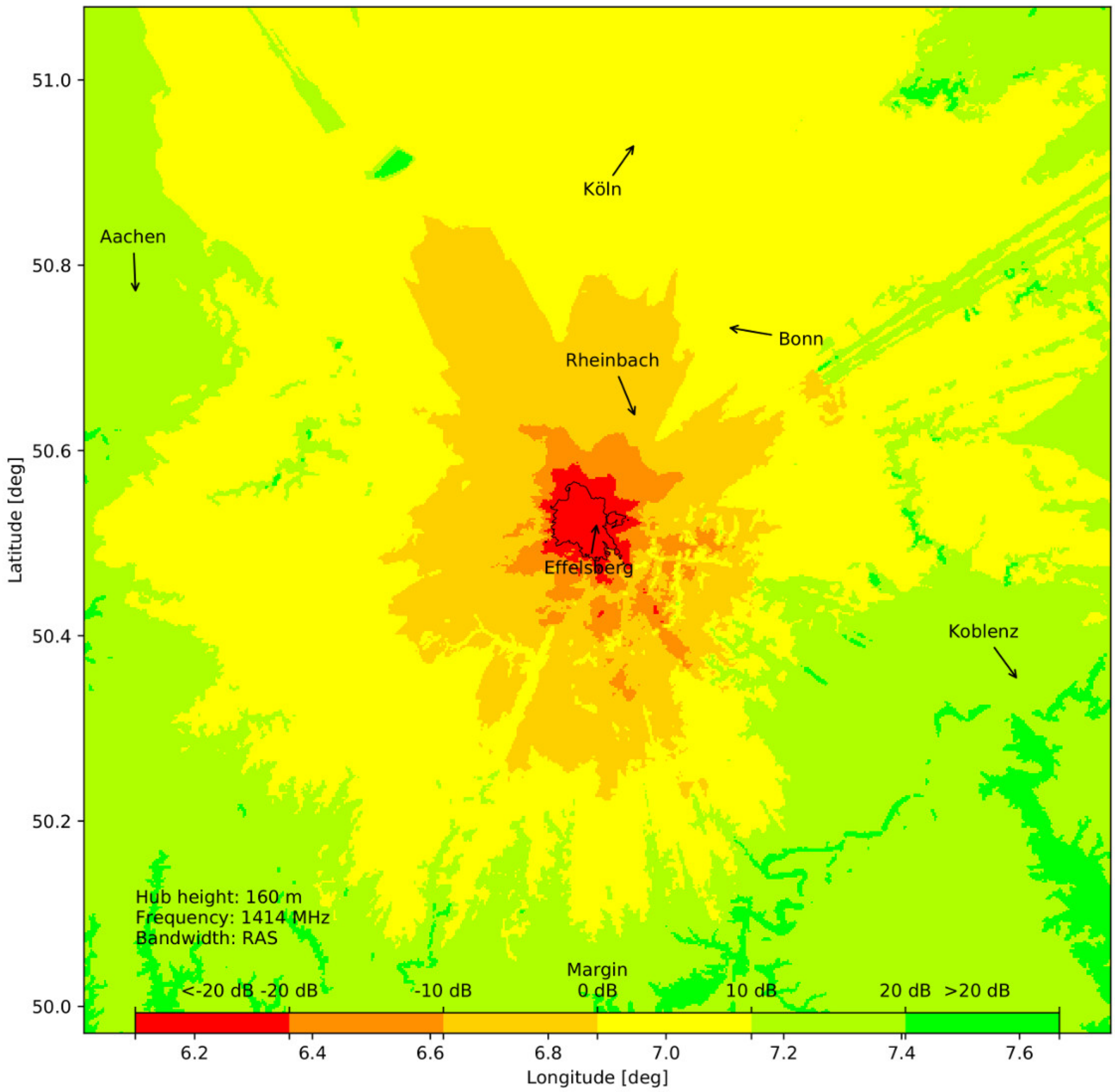

Figure 7: Margins for wind turbines with emissions up to the CISPR-11 limit at $\nu = 1420$ MHz and a hub height of 160 m. The critical areas below 0 dB margin have been coloured in red and orange, while positive margins are indicated with yellow and green. The (radio-wave) horizon (as seen from the telescope centre) is indicated with a black contour

2.4 MEASUREMENT OF THE RADAR CROSS SECTION OF A WIND TURBINE

Where space is available usually a combination of wind turbines and PhotoVoltaic (PV) installations also called solar farms is deployed. This creates an interesting interference scenario because not only the direct radiation from the wind turbines and direct radiation from the PV installation poses a threat but also the radiation from the PV installation reflected by the wind turbines. Other radiators near the wind turbine may also be reflected through the wind turbine. To have an idea about this effect it is necessary to measure the radar cross section of the wind turbine in its actual deployed state. Annex 4 describes a simple method to measure the radar cross section of a working wind turbine.

3 CONCLUSIONS

Although the goal of this Report is to collect measurement methods and discuss the experiences of several individual institutes, and the methods in the respective annexes are the responsibility of the annex authors, some general conclusions may be made:

- It is necessary to investigate the topology of the terrain around a radio astronomy telescope in order to choose the right propagation model. A single radio telescope situation also cannot be used as a template for other studies. A proper propagation model and suitable terrain database should be used;
- The equipment needed for measuring the emissions of a wind turbine goes well beyond the capabilities of regular EMC and monitoring measurement equipment. Custom solutions based on available standard equipment are however not impossible. The actual environment in which the measurements are performed needs to be assessed;
- Wind turbines are, in a number of countries, deployed together with solar panel installations, in order to assess the effect of reflections the RCS of a wind turbine needs to be measured. After this, the cumulative effect of the turbines and PV installations can be better determined.

ANNEX 1: MEASUREMENT SYSTEM FOR THE MEASUREMENT OF VERY LOW EMC LEVELS TO PROTECT THE RADIOASTRONOMY IN THE FREQUENCY RANGE 20-240 MHZ

The method for measuring low EM emissions from wind turbines poses a number of challenges. First, there is the problem that measurements need to take place at considerable distance to be in the far field and there is for these relative low frequencies also the presence of local interferers and the astronomical objects which need to subtracted from the very low EMC radiation of the wind turbines.

The projected windfarm causing most expected issues is located at "Drentse Monden" as indicated in the below figure. Black dots are the locations of wind turbines and the red dot is the LOFAR "Superterp" location.

Figure 8: LOFAR and wind turbine geography

The measurement method involves the use of a multichannel receiver and antenna array functioning as an interferometer to measure the wind turbines emissions and at the same time to eliminate local RF sources and natural sources from the sky. Measurements are performed at a medium distance of 1000 m, this is still in the near field of the wind turbine but the large footprint of the antenna array and processing is able to compensate for this. This method is also capable to subtract local "non wind turbine" interferers and celestial sources from the measurement. A scientific paper with a detailed description of the system is in development. This information may be considered in an addendum of the present Report.

ANNEX 2: MEASUREMENTS AND MEASUREMENT METHODS FOR THE PROTECTION OF THE RADIO ASTRONOMY SERVICE IN THE FREQUENCY RANGES 608-614 AND 1400-1427 MHZ

A2.1 BACKGROUND AND MOTIVATION

In the vicinity of the Radio Telescope Effelsberg in Germany, several wind turbines (WT) were planned. It was to be determined whether unwanted emissions especially from the hubs of these wind turbines may cause interference to the 100 m dish of the radio telescope. Calculations resulted in a considerable interference potential if the emissions from the wind turbines would reach the limits given in CISPR-11 [20]. The distance between radio telescope and planned wind turbines was about 8 km. Although the Radio Telescope Effelsberg is located in a valley providing good natural shielding to the surrounding interference sources, there is a line of sight to the hubs of the wind turbines being 145 m high.

The lowest exclusive band for radio astronomy where the noise level is low enough to allow observations with reasonable sensitivity, and the protection criteria of Recommendation ITU-R RA.769 [15] can be applied, is the frequency range 608 to 614 MHz. The next higher exclusive band is from 1400 to 1427 MHz. Since emission levels from electrical and electronic devices decrease with frequency, measurements were focussed on the above frequency bands. It can be assumed that if protection from harmful interference due to wind turbine emissions in these bands is sufficient, it will also be the case for all higher radio astronomy bands.

The aim of these measurements was to determine typical emission levels from modern wind turbines in the frequency ranges around 611 MHz and 1413 MHz.

A2.2 PROPERTIES OF THE RADIO TELESCOPE EFFELSBERG

The receiving dish of the Radio Telescope Effelsberg has a diameter of 100 m and a Gain of 80 - 90 dBi. However, it was assumed that it will never be pointed directly at a wind turbine. Therefore, emissions from the wind turbines will arrive through a side lobe of the dish for which a gain of 0 dBi was assumed (see Recommendation ITU-R RA.769 [15]). The actual gain under all circumstances in the direction of the wind turbines would have to be considered when their locations for potential implementation are known, which is usually not done for practical reasons. Nevertheless, extremely low noise amplifiers being cooled down to 15 K and observations with extremely long integration time allow the detection of emissions that are more than 50 dB below the thermal noise level.

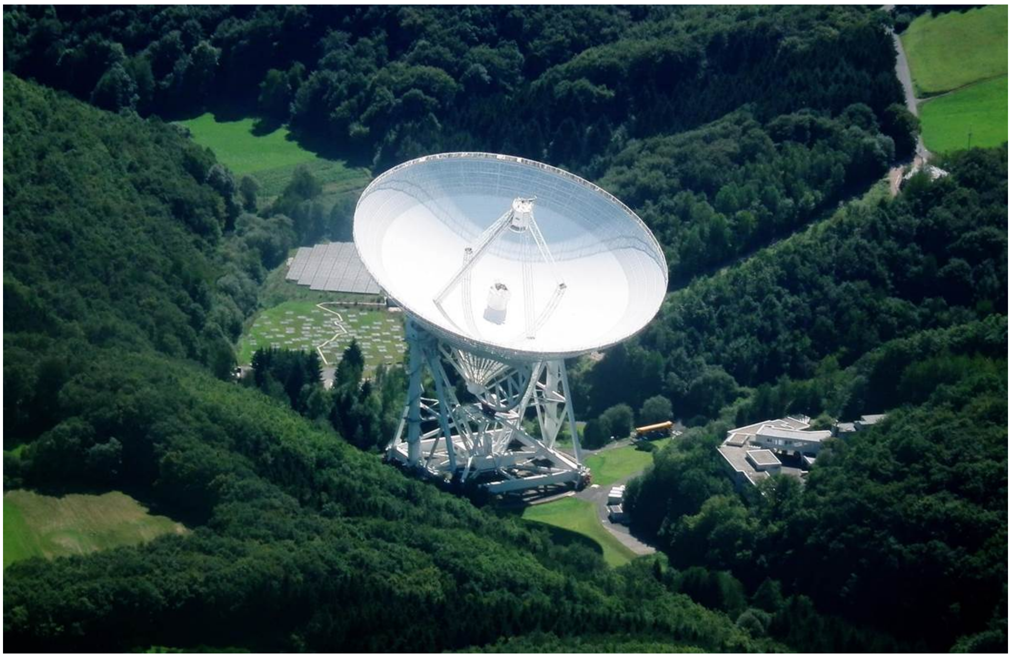

Figure 9: Radio Telescope Effelsberg

A2.3 MEASUREMENT CONCEPT

A wind turbine's potential interference sources are either at the base of the tower or in the hub or nacelle. The rotor blades of modern wind turbines are typically fitted to a tower of 150 m. It would easily be possible to detect emissions from the base on the outside at short measurement distances, but these emissions bear little interference potential as they would be attenuated considerably by the topology and morphology along the way to the radio telescope. The emissions at rotor blade level are therefore of primary interest. The shortest measurement distance possible without any additional equipment (e.g. crane) is 150 m. If the unwanted emissions turned out to be within the tolerable range (30 dB below the limits defined in EN 55011 [21] and EN 61000-6-3 [22]), their level would be well below the inherent noise level of the Monitoring Service's receiving system (receiver plus preamplifier) and would thus not be measurable by conventional means. It was therefore necessary to develop a measurement concept based on procedures similar to those of radio astronomy measurements for measuring RF levels well below the system noise.

The measurement concept used for determining realistic compatibility distances between wind turbines and radio telescopes consisted of five stages:

1 Increasing the measurement system's minimum sensitivity:
Development of a method allowing very weak (interfering) signals to be measured, including those below the measurement system's inherent noise level. This stage included the empirical determination of the optimal integration time and bandwidth for the measurement.

2 Qualitative measurement of the spurious emission pattern of typical wind turbines:
Recording the spurious emissions actually in and on the nacelle and also at the base of large modern wind turbines. The aim was to identify the emissions' pattern (pulsed, continuous, etc.) so as to be able to determine with the help of this information the optimal settings for subsequent quantitative level measurements so that the measurement system would have a maximal sensitivity.

3 Quantitative measurement of the interfering field strengths in the vicinity of wind turbines:
At this stage, an effort was made to determine the interfering field strength of typical modern wind turbines in their immediate surroundings using the optimum receiver settings determined above.

4 Calculation of wind turbines' power density:
At this stage, the radiated disturbance power emitted by wind turbines was calculated from the field strength measured earlier, using the free-space equation. To enable a direct comparison with the tolerable interfering level of the radio telescope given as power density, the disturbance power was also converted into a (fictitious) power flux-density at the interference source (rotor blade).

5 Calculation of the compatibility distances:
At this stage, the average distance needed between wind turbines and radio telescopes at which turbines' RF radiation just no longer causes any interference was calculated. This was done by calculating the extent to which the power flux-density decreases with distance with the help of propagation prediction software. The propagation models were based on the internationally established method described in Recommendation ITU-R P.452 [3]. The topography was taken into account. The point at which the power flux-density decreased to a level at which it just fails to cause any interference to the radio telescope corresponds to the minimum distance at which wind turbines may be installed without interfering with radio astronomy. Annex 3 provides details on the calculation of compatibility distances.

A2.4 SELECTION OF THE MEASUREMENT EQUIPMENT

A2.4.1 Receiver

A real time analyser was used for all measurements as it can cover an RF bandwidth of up to 110 MHz and at the same time store the entire measurement span in the form of I/Q data. It had a noise figure of 4 dB.

A2.4.2 Preamplifier

A broadband preamplifier covering the range 10 MHz to 3 GHz was used. It had a noise figure of 1.2 to 2 dB and a gain of about 19 dB in the frequency ranges to be measured. This meant that the inherent noise of the entire set-up consisting of preamplifier and receiver was more or less identical to the amplifier noise (max. 2 dB).

The system sensitivity is influenced, but not directly dependent on the overall noise figure. It is obvious that lower noise figures improve system sensitivity, but since the level of external signals are obtained by subtracting the system noise from the measured total power of system noise and external signals, the time and temperature stability of the system is finally limiting the lowest external signal power that can be measured (see section A2.8).

A2.4.3 Antennas

Antennas with the highest possible directivity and the highest possible gain in the direction of maximum radiation were needed for the measurements. In view of the measurement antennas that were available, it was decided to use a mobile dish fixed to a tripod for the 1.4 GHz range.

Initially it had been decided to opt for a log periodic antenna for the 610 MHz range. However, the measurements revealed that the directivity and gain of the log periodic antenna in the 610 MHz range did not suffice to differentiate between the components from the wind turbines and the radio noise and interference in the environment. A 15-element-Yagi-antenna was therefore used in later measurements.

The main characteristics of the antennas used are listed in the below table.

Table 1: Characteristics of the measurement antennas

	Log periodic	Dish	Yagi
Frequency range	400-3600 MHz	1 GHz – 18 GHz	470-790 MHz
Gain	6.5 dBi	17.2 dBi	12.8 dBi (at 611 MHz)
Antenna factor K	17.3 dB(1/m) → 611 MHz	13.9 dB(1/m) → 1413 MHz	11 dB(1/m) → 611 MHz
3 dB opening angle	ca. 60°	< 20°	25°

A2.4.4 Filter

At some measurement locations, signals from DVB-T transmitters in neighbouring channels were very strong, so that overloading of the Receiver/LNA combination was possible. Therefore, a tuneable 5 cavity band pass filter was inserted between antenna and LNA for noise measurements at 611 MHz. The filter was tuned to the radio astronomy band.

A2.5 MEASUREMENT OF THE EMISSION CHARACTERISTICS

If the spurious emissions are not similar to noise but consist, for example, of short, very broadband pulses or continuous carriers, it is possible to increase the sensitivity of the measurement set-up by optimising the settings of the measurement bandwidth. The signal-to-noise ratio rises with increasing measurement bandwidth in the case of broadband pulses whereas in the case of narrowband signals or even continuous carriers the ratio increases as the measurement bandwidth decreases.

To determine typical spectral characteristics of modern wind turbines, measurements were conducted at two common types of wind turbine from major vendors. The measurements were carried out at the base in the towers and both in and on top of the nacelle (hub). A handheld direction-finding antenna was used for the measurements. No quantitative measurement of the interference power was planned at these measurement points. At any case, this would not have been possible because of the unknown distance to the interference source and the unknown attenuation of any emission sources inside the nacelle by its housing. However, it was assumed that any interfering signals measured so close to potential emission sources would be immediately visible in the spectrum, thereby revealing their spectral characteristics.

To be able to trace the source of the signals, a measurement was carried out during two different operating modes:

- motionless rotor blades, all electronic components switched off;
- turbine in operation with rotating blades and electricity being exported to the local electricity grid network.

Figure 10: Measurements of the signal characteristics directly at the sources

These measurements showed no characteristic emissions that are pulsed or consisted of single carriers in the investigated frequency ranges. The only significant emissions were broadband and continuous, so that a special adjustment of the measurement bandwidth was not relevant. As an example, the below figure shows the recording of a noise-like emission from the automatic rotor blade angle adjustment.

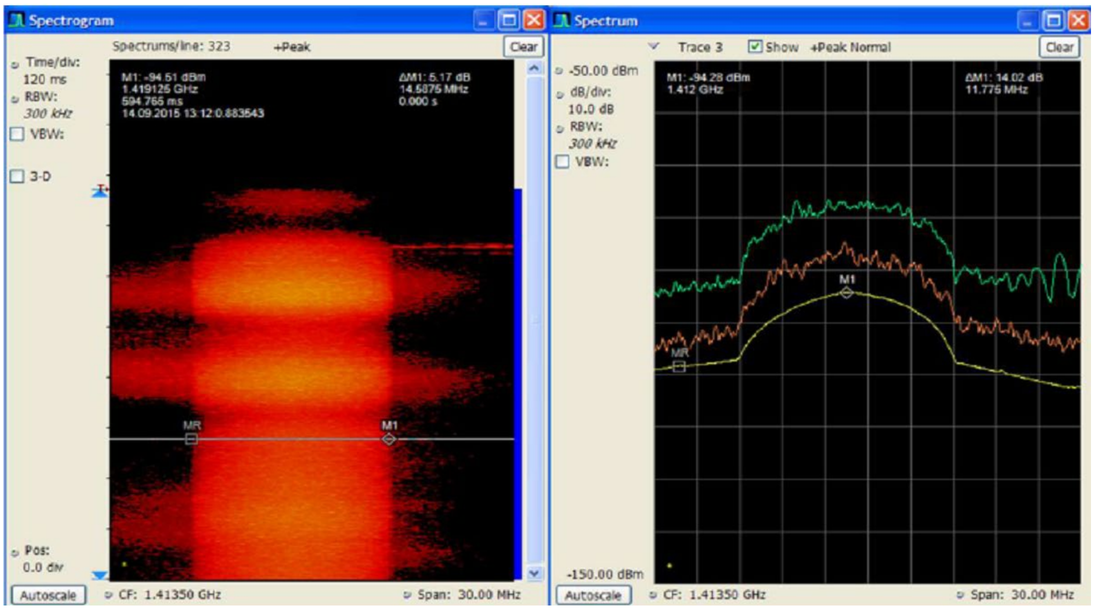

Figure 11: Emissions from a wind turbine hub

The left panel shows time vs. frequency over a period of 1 s with levels displayed in different colour, the right panel shows level vs. frequency in PeakHold (green), momentary (red) and average (yellow) mode.

A2.6 MEASUREMENT PARAMETERS

As a result of the measurements near the emission sources and the properties of the available equipment, the following parameters were selected for the actual emission level measurements:

Table 2: Measurement parameters

Parameter	at 611 MHz	at 1413 MHz
Centre frequency	611 MHz	1413 MHz
Captured data	I/Q samples	I/Q samples
Capture bandwidth	1.25 MHz	10 MHz
Detector	RMS	RMS
Capture/integration time	85 s	20 s

A2.7 MEASUREMENT OF THE SYSTEM NOISE

As said in Section A2.4 of this Report, measurement of noise-like signals below the system noise level are possible when separately measured levels of external and system noise are integrated over a long time and subtracted in linear units.

One prerequisite for this method is the knowledge of the exact system noise level and the optimum integration time. The optimum integration time is determined by the temperature stability of the level measurement.

If the integration time is too long, temperature drifts of the receiver components take over and increase the measurement error. The optimum integration time is determined by a long-term registration of the momentary system noise levels when the input of the system is terminated. The total registration time is divided into a certain number of integration intervals. The average noise level in each integration interval is compared with that of the next interval. The result is the so-called "Allan variance" which is calculated by the following formula:

$$\sigma_A^2(\tau) = \frac{1}{2\cdot(n-1)}\cdot\sum_{k=1}^{n-1}\left(\frac{\overline{P}_{k+1}(\tau)-\overline{P}_k(\tau)}{\overline{P}}\right) \qquad (2)$$

Where:

- σ_A^2 is Allan variance;
- τ is integration time in s.

The optimum integration time is where σ_A^2 is at its minimum. The following example shows the results of such a measurement.

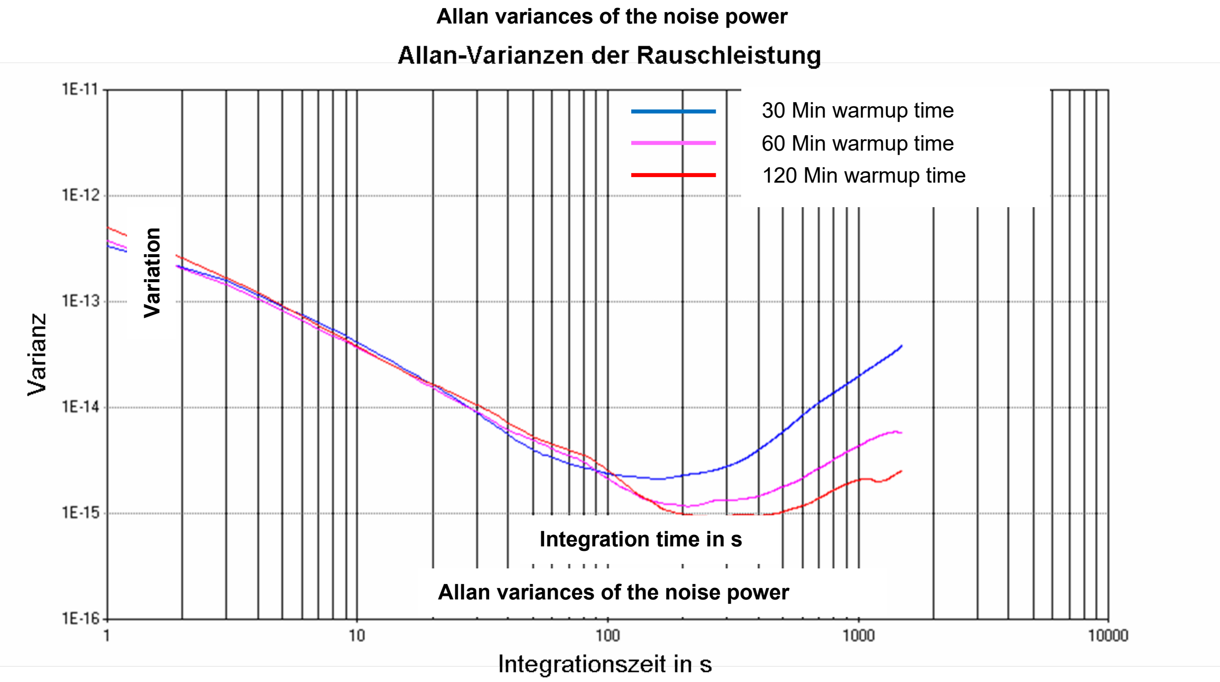

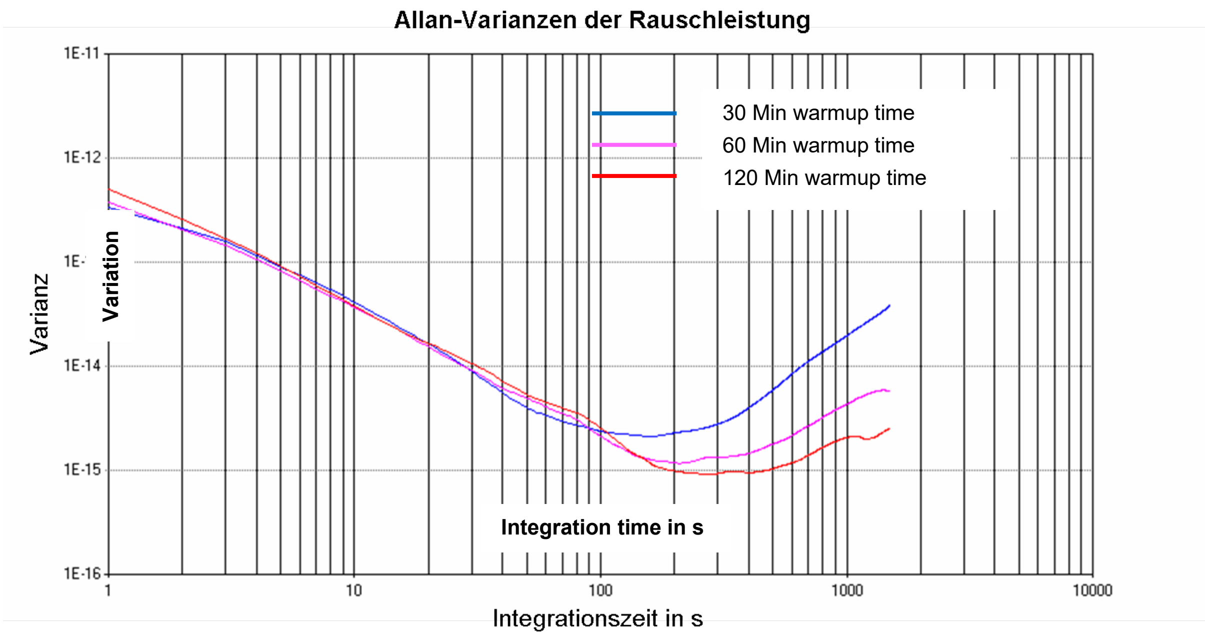

Figure 12: Drift of the average noise level at different integration times

It can be seen that in this example the maximum accuracy is achieved with an integration time between 200 and 400 s after a warmup time of 120 min. However, the maximum storage capacity for I/Q samples of the used analyser at 1.25 MHz bandwidth was limited to 85 s, and at 10 MHz bandwidth the maximum was 20 s, so those were the integration times used. The left part of the curves reveals an exponential decrease (linear in a double-logarithmic plot). This is owing to the radiometer equation, which predicts a decrease of the system noise with the square root of the integration time. As with many broadband measurement receivers, the used real time analyser had an internal alignment procedure that is called automatically every few minutes. The below figure shows the momentary system noise level over a time period of 85 s, starting immediately after an alignment procedure.

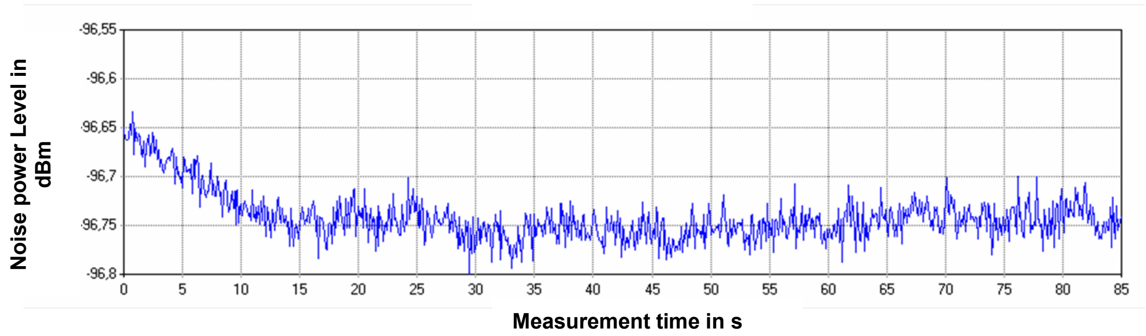

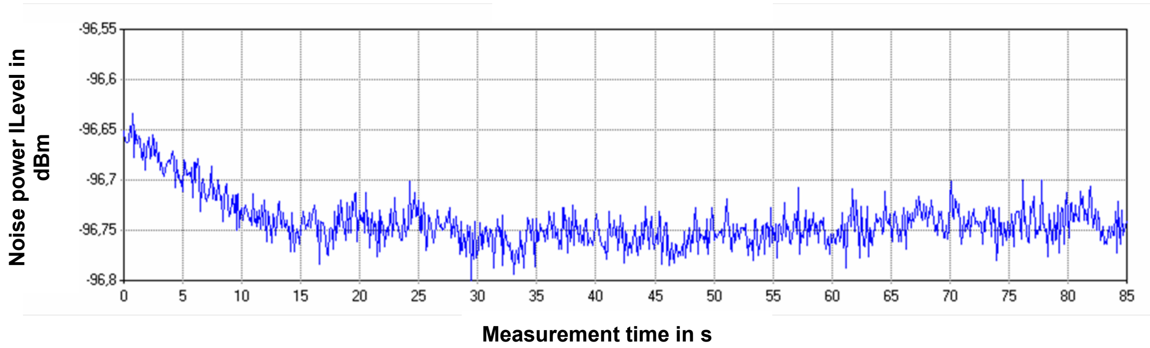

Figure 13: Time drift of the measured noise level after alignment

It can be seen that the time drift of the level indication stabilizes after about 15 s, so all measurements were started only with this delay after alignment.

A2.8 EXTERNAL NOISE MEASUREMENT

To gain an overview of typical emission levels from currently installed wind turbines in Germany, measurements were performed at three different locations with wind turbines of different types from three major vendors. The total noise power was measured as described in Section 2 of this Report, with the antenna positioned about 150 m away from the pole of the wind turbine and pointing to different directions:

a) Towards the wind turbine hub ("on-position");

b) Away from the wind turbine and away from the sun ("off-position");

c) Away from the wind turbine but towards the sun ("sun-position").

In all three measurements, the elevation was equal (about 45°). The azimuths of the measurements were about 90° apart.

The sun-position was measured at some locations to determine its noise level compared to the emission levels of other noise sources.

Figure 14: Measurement of wind turbine emission levels (left: at 611 MHz, right: at 1413 MHz)

Figure 15: Map of a wind turbine with "on" and "off" directions. Purple: measurement location

Prior to the measurements it was ensured that no dominant radio noise sources such as overhead high voltage lines or electric train installations were in the vicinity, both in on and off-directions of the antenna. During the measurements, the wind turbines were running.

During the integration time (measurement duration), all samples were recorded, and the average power calculated. For clarity, a diagram was drawn up, illustrating the average power level at 200 ms intervals. The below figures illustrate the results of measurements obtained in front of a wind turbine.

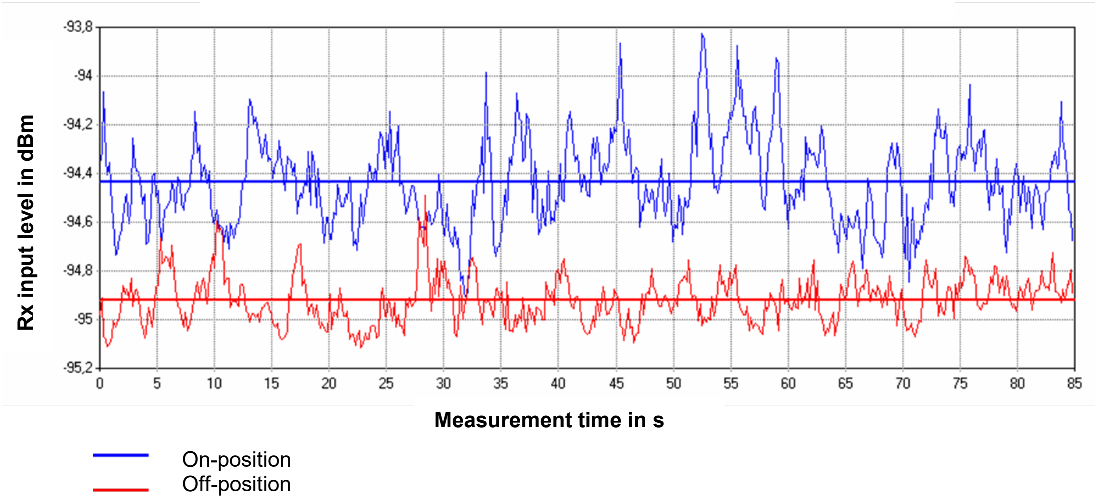

Figure 16: Noise level in front of wind turbine #2 at 611 MHz

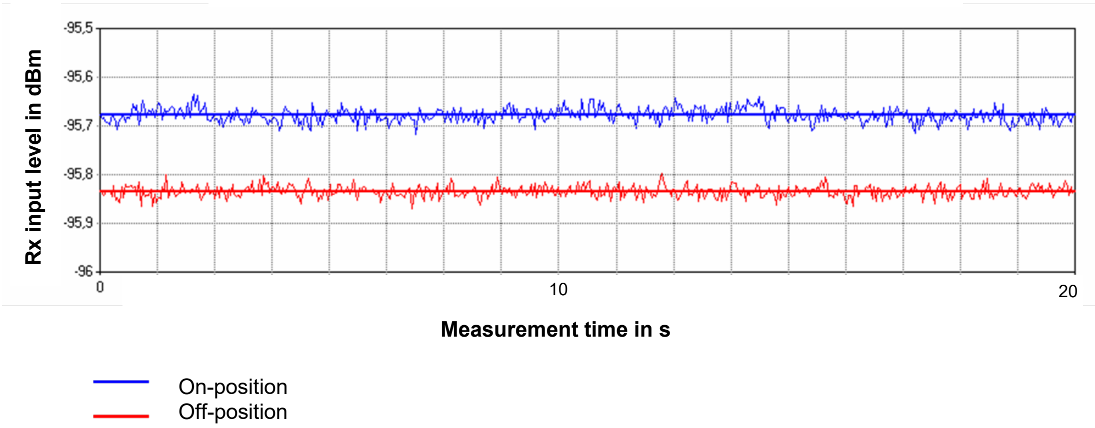

Figure 17: Noise level in front of wind turbine #2 at 1413 MHz

The contribution to the noise level at the measurement point emitted by the wind turbine was obtained by calculating the difference in the measurements in the on- and off-position:

$$P_{WT} = P_{ON} - P_{OFF} \text{ (all levels in linear units)} \quad (3)$$

This equation assumes that all other RF contributions at the measurement receiver (especially inherent noise and man-made noise) remain stable and do not change during the on- and off-positions. It was noted that the levels in the direction of the wind turbines occasionally fluctuated more strongly during the on-position measurement. The below table shows the resulting Rx input levels at the three measured wind turbines, always normalised to 1 MHz bandwidth. These measurements were done with the Log periodic antenna at 611 MHz.

Table3: Rx levels at the measured wind turbines

	Wind turbine #1		Wind turbine #2		Wind turbine #3	
Rx input level	at 611 MHz	at 1413 MHz	at 611 MHz	at 1413 MHz	at 611 MHz	at 1413 MHz
P_{ON}	-94.48 dBm	-95.68 dBm	-94.23 dBm	-95.68 dBm	-81.73 dBm	-87.36 dBm

	Wind turbine #1		Wind turbine #2		Wind turbine #3	
P_{OFF}	-94.08 dBm	-95.71 dBm	-94.72 dBm	-95.84 dBm	-81.47 dBm	-87.40 dBm
P_{WT}		-117.15 dBm		-110.20 dBm		-107.04 dBm

Note: It has to be noted that if the P_{ON} and P_{OFF} values corresponding to the measurements on the noise floor with and without the wind turbines are significantly higher than the calculated P_{WT} as is the case in table 3 then the measurement device requires an accuracy suitable for the small measured differences.

From above table, it can be concluded that the wind turbine is not always the dominant interferer in the existing environment.

A2.9 ADDITIONAL MEASUREMENTS AT 611 MHZ

The evaluation of the first measurements at 611 MHz revealed a higher overall level in the off-position than in the on-position at two of the three locations. Since it had been possible to determine and reproduce the measurement system noise accurately during preliminary measurements, it had to be assumed that the remaining external noise or interference components differed in the on- and off-positions. This implies that at a distance of about 200 m, the spread in time depending on the direction of the unwanted noise components in this frequency range is higher than the overall interference power of the wind turbine.

Unlike the parabolic reflector at 1400 MHz, the directivity discrimination of the log periodic antenna used did not suffice to capture just that part of the radio noise emanating from the direction of maximum radiation, even at the chosen elevation of 45°. It is therefore assumed that parts of nearby interference sources added a measurable contribution to the radio noise from a horizontal direction. This also applied to the spurious emissions or sidebands of adjacent DVB-T transmitters, the field strengths of which were very high at some of the measurement locations.

To solve this problem, further measurements were carried out with a Yagi antenna normally used by the Monitoring service for the TV band. At 611 MHz the Yagi antenna has a higher gain and a narrower aperture than the log periodic antenna used for the initial measurements.

As at 600 MHz the unwanted noise components, like the MMN, are much stronger than at 1400 MHz and penetrate the receiver noise band, it was possible to apply a simplified measurement principle to the additional measurements. The mean channel power was measured in a 1 MHz and 10 MHz band around the centre frequency of the radio astronomy band at 611 MHz for an integration time of 1 s. In each second, the measurement receiver averaged 1.25 million measured values (spectrally and in time) to a single RMS value.

The levels of 14 different wind turbines were measured during this additional measurement campaign.

Since it was likely that the Sun’s radiation would be stronger than the other radio noise components and those received from the wind turbines, the antenna orientation was altered at least four times at each measurement location:

- in the direction of the wind turbine (on-position);
- in the direction of the sun;
- abeam the sun and the wind turbine (off-position 1, 2, …).

The position of the vehicle with the measurement set-up was such that the directivity discrimination between the wind turbine and the sun was at least 90°. Direction-wise, the off-positions were in the middle between the sun and the wind turbine. The measurement antenna’s elevation was set to about 40°. The slant range between the measurement antenna and the nacelle of the wind turbine being measured varied between 135 and 250 m.

The measurements revealed that the levels received varied at the different locations, both in the on- and the off-positions. The differences in the levels exceeded the measurement receiver’s or preamplifier’s drift over temperature. It was therefore assumed that these differences were caused by the difference in the levels of the various noise components, including those of the wind turbine. Such differences lead to a lower sensitivity threshold when calculating the external radiation levels. The evaluation of the receiving levels in (at least 2) different off-positions at each measurement site showed that the stability of the unwanted noise components could not possibly be better than 0.1 dB. This implied that differences in the levels at different antenna orientations at a single site of less than 0.1 dB should be deemed negligible. This yielded a measurement sensitivity of:

$$P_{min} = P_{off} - 10\log_{10}\left(10^{(P_{off}+0.1)/10} - 10^{P_{off}/10}\right) = P_{off} - 16.33\text{ dB} \quad (4)$$

The lowest verifiable P_{min} level of external noise components from a wind turbine (or the sun) was hence calculated to be 16.33 dB below the lowest P_{off} level measured during an off-position.

An example of the evaluation of the values measured in front of a wind turbine is shown in the below table. The column “additional Rx level” relates to the receiving level of the external noise component in addition to that of the noise in the off-position. This level was calculated with the help of the reading P_{meas} as shown below:

$$P_{add} = 10\log_{10}\left(10^{\frac{P_{meas}}{10}} - 10^{\frac{P_{off}}{10}}\right) \quad (5)$$

The column “additional Rx level at antenna“ shows the power flux-density in a 1 kHz bandwidth at the base of the measurement antenna. It was derived from the previous column as follows:

$$P_{1Hz} = P_{add} - 10\log_{10}\left(\frac{measurementBW}{1\text{Hz}}\right) + v \quad (6)$$

where *v* is the overall attenuation of the measurement set-up resulting from cable and filter attenuation and the preamplifer’s amplification. In this example, *v* = -12.6 dB, i.e. the preamplifier’s amplification exceeds cable and filter attenuation.

Table 4: External noise measurements at 611 MHz with Yagi antenna

	In measurement bandwidth		In 1 Hz bandwidth at measurement antenna (note 1)	At isotropic Antenna	(Note 2)
Measurement Direction	**Reading**	**Additonal Rx level**	**Additional Rx level**	**Addtional Rx level**	**!**
213°, towards wind turbines	-91.74 dBm	-108.07 dBm	-180.7 dBm/Hz	-193.5 dBm/Hz	<
311°, Sun	-91.64 dBm	-106.63 dBm	-179.2 dBm/Hz	-192.0 dBm/Hz	
130°, off-position 1	-91.78 dBm	-108.11 dBm	-180.7 dBm/Hz	-193.5 dBm/Hz	<
50°, off-position 2	-91.76 dBm	-108.09 dBm	-180.7 dBm/Hz	-193.5 dBm/Hz	<

Note 1: The column "additional Rx level at isotropic antenna" is the additional power of the external noise component at a (fictitious) isotropic radiator. It is derived from the column on the left by deducting the 12.8 dBi gain of the measurement antenna.

Note 2: Where the differences in the levels measured between the wind turbine/sun and the off-positions is smaller than 0.1 dB, the value in the table has been marked with red and with "<". It means that the real value of the radiation component could not be measured and is below the value indicated.

The measurement revealed that at nearly all measurement sites the highest level was measured in the direction towards the sun, followed by that in the direction of the wind turbine. The levels were always slightly higher than those in the off-positions.

The below table shows the receiving levels measured at 611 MHz at all wind turbine sites at which measurements were carried out.

Table 5: External noise levels at all measured wind turbines at 611 MHz

Location / WT	Reading	Additional Rx level in 1 Hz Bw at isotropical antenna (P_{WEA})
Lamerdingen	-81.23 dBm	-193 dBm
Landshut	-91.90 dBm	-192 dBm
Oberwaltenkofen	-91.73 dBm	< - 193 dBm
Dietrichsdorf	-91.76 dBm	< -193 dBm
Sünzhausen	-91.67 dBm	< -193 dBm
Paunzhausen	-91.97 dBm	< -194 dBm
Weißling (measurement 1)	-91.74 dBm	< - 193 dBm
Weißling (measurement 2)	-91.68 dBm	< -193 dBm
Dachau	-91.74 dBm	< -193 dBm
Odelzhausen 1	-92.10 dBm	< -194 dBm
Odelzhausen 3	-92.01 dBm	< -194 dBm
Odelzhausen 4	-91.97 dBm	< -194 dBm
Odelzhausen 5	-91.90 dBm	< -194 dBm
Dasing 1	-92.13 dBm	< -194 dBm
Dasing 2	-92.16 dBm	< -194 dBm
Dasing 3	-92.16 dBm	< -194 dBm

The level increase in the direction of the wind turbine relative to the off-position exceeded 0.1 dB at only two sites and as such was verifiable. The measured wind turbine interference levels were hence very low.

A2.10 CALCULATION OF THE EMITTED RF POWER FLUX DENSITIES OF THE WIND TURBINES

First, the calculated wind turbine receiving levels in the measurement bandwidth under study were converted into spectral power density by means of bandwidth conversion:

$$P_{EIRP,\mathrm{dB}}/\mathrm{Hz} = P_{EIRP,\mathrm{dB}} - 10\log_{10}\left(\frac{B}{\mathrm{Hz}}\right) \quad (7)$$

Using free-space propagation and the attenuation levels given in the level plan below, it was possible to calculate the radiated power of the disturbance P_{EIRP} from the spectral power densities measured at the site.

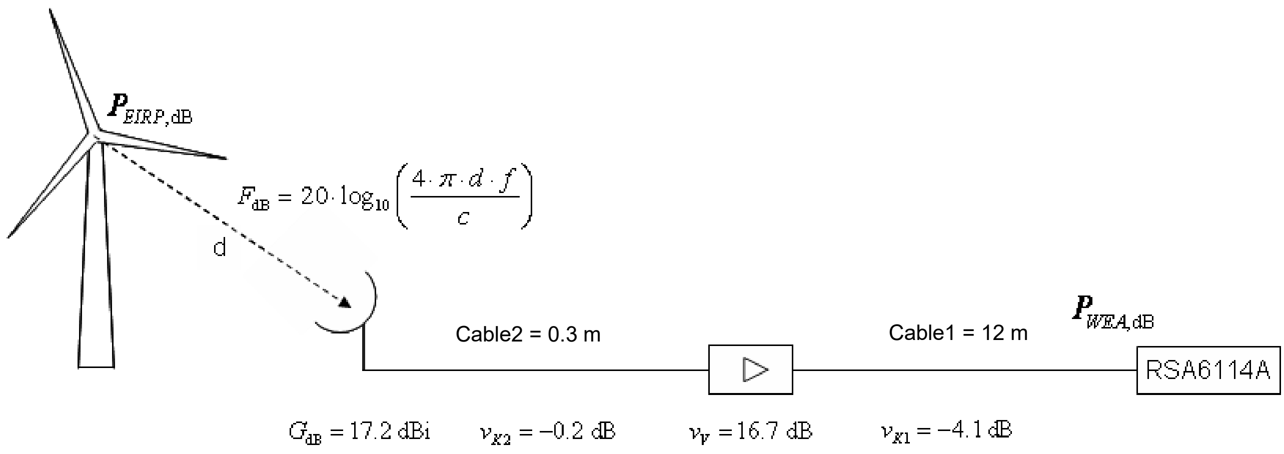

Figure 18: Level plan of the measurement setup at 1413 MHz

The emitted RF power from the wind turbine was:

$$P_{EIRP} = P_{WT} - v_v - v_{K1} - v_{K2} - G + F \tag{8}$$

The corresponding values for the wind turbines measured at 1413 MHz are given in the below table.

Table 6: Measured and emitted power flux density of the wind turbines at 1413 MHz

	Type 1	Type 2	Type 3
Measured Rx level: $P_{WEA,dB}$	-147.15 dBW	-140.19 dBW	-137.04 dBW
Measured bandwidth: B	1.25 MHz	1.25 MHz	10 MHz
Distance to wind turbine: d	202 m	196 m	192 m
Free-space loss: F_{dB}	81.55 dB	81.3 dB	81.12 dB
Emitted power in meas. Bw: $P_{EIRP,dB}$	-95.0 dBW	-88.49 dBW	-85.52 dBW
Emitted pfd: $P_{EIRP,dB}/\mathrm{Hz}$	-156.17 dBW/Hz	-149.46 dBW/Hz	-155.52 dBW/Hz

The following table shows the corresponding values for the wind turbines measured at 611 MHz during the second measurement campaign. The manufacturer data have been made anonymous.

Table 7: Measured and emitted power flux density of the wind turbines at 611 MHz

Location / WT	Vendor / Type	Rx level PWEA/Hz	Meas. distance	Free-space loss	Emitted power flux density
Lamerdingen	1	-193 dBm	200 m	74.1 dB	-149 dBW/Hz
Landshut	2	-192 dBm	200 m	74.1 dB	-148 dBW/Hz
Oberwaltenkofen	3	< - 193 dBm	135 m	70.8 dB	< -153 dBW/Hz
Dietrichsdorf	4	< -193 dBm	155 m	72.0 dB	< -151 dBW/Hz

Location / WT	Vendor / Type	Rx level PWEA/Hz	Meas. distance	Free-space loss	Emitted power flux density
Sünzhausen	4	< -193 dBm	250 m	76.1 dB	< -147 dBW/Hz
Paunzhausen	4	< -194 dBm	208	74.5 dB	< -149 dBW/Hz
Weißling (measurement 1)	4	< - 193 dBm	238 m	75.7 dB	< -148 dBW/Hz
Weißling (measurement 2)	4	-193 dBm	238 m	75.7 dB	< -148 dBW/Hz
Dachau	4	< -193 dBm	250 m	76.1 dB	< -147 dBW/Hz
Odelzhausen 1	1	< -194 dBm	243 m	75.9 dB	< -148 dBW/Hz
Odelzhausen 3	1	< -194 dBm	208 m	74.5 dB	< -149 dBW/Hz
Odelzhausen 4	1	< -194 dBm	172 m	72.9 dB	< -151 dBW/Hz
Odelzhausen 5	1	< -194 dBm	206 m	74.5 dB	< -149 dBW/Hz
Dasing 1	1	< -194 dBm	200 m	74.2 dB	< -150 dBW/Hz
Dasing 2	1	< -194 dBm	200 m	74.2 dB	-150 dBW/Hz
Dasing 3	1	< -194 dBm	180 m	73.3 dB	< -151 dBW/Hz

In summary, the maximal spectral power density level of the wind turbines was -148 dBW/Hz at 611 MHz range and -149.5 dBW/Hz at 1413 MHz.

A2.11 COMPARISON WITH EMC LIMITS

For assessing the radiation levels, the measured values should be compared with the limit in EN 55011 (Table 5) [20] and EN 61000-6-3 [21], although this limit only applies to the frequency range up to 1 GHz. The limit is defined as a quasi-peak field strength of 37 dBµV/m in a measurement bandwidth of 120 kHz at a standard distance of 10 m to the radiation source. However, this value applies only under laboratory conditions. Table 17 in EN 55011 specifies that this limit also applies at the site of operation at a distance of 30 m. This differential is also assumed for the values in EN 61000-6-3. The measured spectral power densities are converted into this field strength as follows:

projecting 1 Hz to 120 kHz:

$$P_{120kHz} = \frac{P_{EIRP}}{Hz} + 10\log_{10}(120000) = \frac{P_{EIRP}}{Hz} + 50.8\ dB \quad (9)$$

converting the RMS to quasi-peak values:

$$P_{Pk} = P_{RMS} + 5.5\ \text{dB} \quad (10)$$

The 5.5 dB conversion factor was determined empirically in the laboratory with white noise. Since measurements at the wind turbine itself did not reveal pure, narrowband, continuous signals or pulses with low pulse lengths/pause ratios, it may be assumed, by approximation, that the radiated disturbance powers from the wind turbine consist of the aggregation from several single sources, which justifies the assumption that the calculated conversion factor is realistic.

Calculating the free-space attenuation at a distance of 30 m:

$$F_{30m,dB} = 20\log_{10}\left(\frac{4\pi 30 f}{c}\right) = \text{ 58 dB (at 611 MHz) or 65 dB (at 1413 MHz)} \quad (11)$$

where c is the velocity of light in m/s and f is the measurement frequency in Hz.

Converting the power level into a voltage level:

$$P_{dB}/dBW = U_{dB}/dB\mu V + 137dB. \quad (12)$$

Converting the voltage level into field strength:

$$E_{dB} = U_{dB} - 20\log_{10}(f) - G_{dB} - 29.78 \quad (13)$$

where f is the measurement frequency in MHz.

Since value U represents the voltage at the connector of an isotropic antenna, equation 11 must be based on a gain of 0 dB.

In combination with the conversion factors obtained in equations 7 to 10, the sum of all constants when converting the spectral power density at a wind turbine into a quasi-peak field strength at a distance of 30 m at 1413 MHz is:

$$50.8\text{ dB} + 5.5\text{ dB} - 65\text{ dB} + 137\text{ dB} + 33.2\text{ dB} = 161.5\text{ dB} \quad (14)$$

and at 611 MHz:

$$50.8\text{ dB} + 5.5\text{ dB} - 58\text{ dB} + 137\text{ dB} + 25.9\text{ dB} = 161.2\text{ dB} \quad (15)$$

The values for the wind turbines measured at 611 MHz (the limit is 37 dBµV/m at a distance of 30 m) are given in the below table.

Table 8: Comparison of measured wind turbine emissions with EMC limits at 611 MHz

Location / WT	Vendor / type	Emitted spectral pfd	Field strength at 30 m dist. (QP/120kHz)	Margin to EMC limit
Lamerdingen	1	-149 dBW/Hz	12 dBµV/m	25 dB
Landshut	2	-148 dBW/Hz	11 dBµV/m	26 dB
Oberwaltenkofen	3	< -153 dBW/Hz	< 8 dBµV/m	> 29 dB
Dietrichsdorf	4	< -151 dBW/Hz	< 10 dBµV/m	> 27 dB
Sünzhausen	4	< -147 dBW/Hz	< 14 dBµV/m	> 23 dB
Paunzhausen	4	< -149 dBW/Hz	< 12 dBµV/m	> 25 dB
Weißling (measurement 1)	4	< -148 dBW/Hz	< 13 dBµV/m	> 24 dB
Weißling (measurement 2)	4	< -148 dBW/Hz	< 13 dBµV/m	> 24 dB

Location / WT	Vendor / type	Emitted spectral pfd	Field strength at 30 m dist. (QP/120kHz)	Margin to EMC limit
Dachau	4	< -147 dBW/Hz	< 14 dBµV/m	> 23 dB
Odelzhausen 1	1	< -148 dBW/Hz	< 13 dBµV/m	> 24 dB
Odelzhausen 3	1	< -149 dBW/Hz	< 12 dBµV/m	> 25 dB
Odelzhausen 4	1	< -151 dBW/Hz	< 10 dBµV/m	> 27 dB
Odelzhausen 5	1	< -149 dBW/Hz	< 12 dBµV/m	> 25 dB
Dasing 1	1	< -150 dBW/Hz	< 11 dBµV/m	> 26 dB
Dasing 2	1	< -150 dBW/Hz	< 11 dBµV/m	> 26 dB
Dasing 3	1	< -151 dBW/Hz	< 10 dBµV/m	> 27 dB

The below table sets out the values for the measured wind turbines at 1413 MHz (the limit is 37 dBµV/m at a distance of 30 m).

Table 9: Comparison of measured wind turbine emissions with EMC limits at 1413 MHz

Location / WT	Vendor / type	Emitted spectral pfd	Field strength at 30 m dist. (QP/120kHz)	Margin to EMC limit
Lamerdingen	1	-156 dBW/Hz	5 dBµV/m	32 dB
Trogen	4	-140 dBW/Hz	12 dBµV/m	25 dB
Friesenried	2	-155 dBW/Hz	6 dBµV/m	31 dB

The radiated disturbance powers of the measured wind turbines were below the limits given in ETSI EN 55011 for 611 and 1400 MHz by at least 25 dB.

A2.12 CALCULATION OF PROTECTION DISTANCES

The maximum tolerable power flux-density level of interference at a radio telescope site is defined in Recommendation ITU-R RA 769-2 [15] for the more sensitive continuum observation (co) mode as follows:

- limit for 611 MHz: -253 dBW/(Hz·m²);
- limit for 1413 MHz: -255 dBW/(Hz·m²).

For a direct comparison with these limits, the power density levels of the wind turbines had to be converted into power flux density. This was done with the following equation:

$$S = \frac{P_{EIRP}/Hz}{A_W} \tag{16}$$

where Aw is the effective area of the isotropic radiator. It was calculated with the following equation:

$$A_W = \frac{\lambda^2}{4\pi} \tag{17}$$

yielding 0.0192 m² at 611 MHz and 0.00358 m² at 1413 MHz.

The difference between spectral power flux-density at the wind turbine site and the limit in Recommendation ITU-R RA.769 [15] must be provided by the path loss. The necessary path loss between wind turbine and radio telescope at which just no interference is caused to the radio telescope is set out in the below table. Only those wind turbines are included in the list which generated the highest interference levels.

Table 10: Calculation of necessary path loss to radio telescope

Parameter	611 MHz (Type 2 in Landshut)	1413 MHz (Type 4 in Trogen)
Emitted pfd: $P_{EIRP,\mathrm{dB}}/\mathrm{Hz}$	-148 dBW/Hz	-149.5 dBW/Hz
Spectral density: S / dB	-131 dBW/(Hz·m²)	-125 dBW/(Hz·m²)
Necessary path loss (co)	124 dB	130 dB

The actual level of the path loss between the planned wind turbine sites around Effelsberg and the radio telescope were calculated using the propagation model given in Recommendation ITU-R P.452-16 [3], due consideration being given to topography. The Max Planck Institute provided files with topographical data about the area surrounding radio telescope Effelsberg. The data had been collected during the 2000 space shuttle mission during which 3D measurements of the Earth were taken. As an example, the below figure shows the outcome of the calculation programme for one of the planned wind turbines.

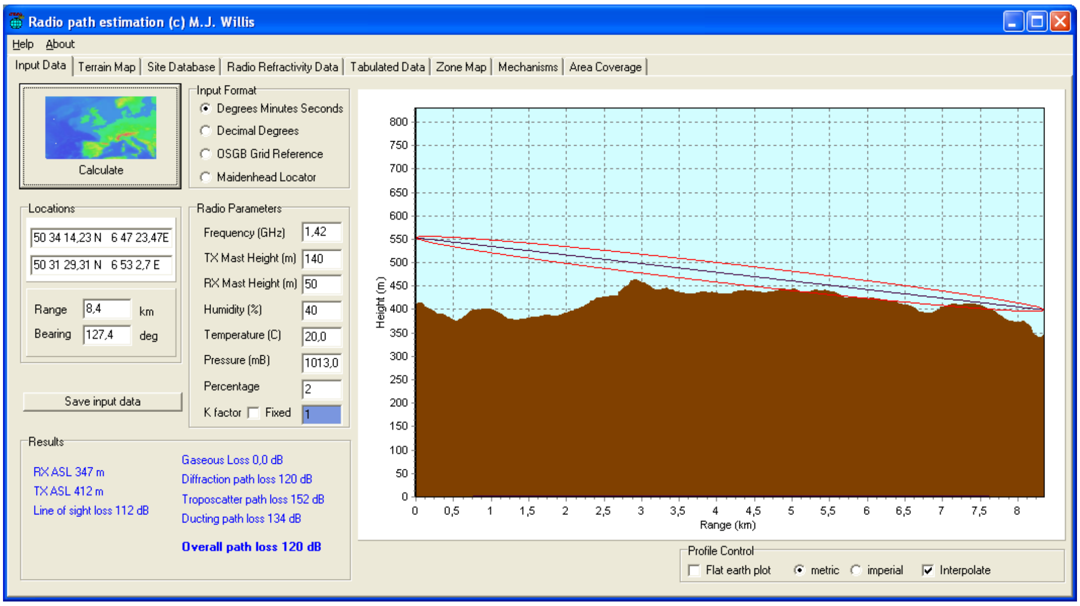

Figure 19: Example of path loss calculation

The below table shows the results of the calculations for the six wind turbines currently being planned.

Table 11: Actual path losses between planned wind turbines and radio telescope Effelsberg

Wind turbine	BAM-46	BAM-47	BAM-48	BAM-49	BAM-50	BAM-51
Path loss at 611 MHz	116 dB	108 dB	106 dB	103 dB	108 dB	112 dB
Path loss at 1413 MHz	120 dB	112 dB	111 dB	111 dB	111 dB	112 dB

The calculations revealed that at all planned sites, there would be a line of sight between the hub of the turbine and the radio telescope's antenna. In some cases even the first Fresnel zone would be (unobstructed). For this reason, the path losses would be approximately equal to the free-space attenuation. The actual path losses would in fact be lower than necessary for interference-free continuum observation (co). The difference between necessary and actual path loss would be more or less the same both in the case of 611 MHz and 1413 MHz.

At the last stage, the propagation calculation programme was used to calculate the area around the Effelsberg radio telescope beyond which interference-free operation of one of the measured wind turbines would be possible. This calculation was based on the wind turbine for which the highest disturbance levels had been measured. The hub was assumed to be located at a height of 140 m. However, it has to be noted that the critical ranges shown here may increase substantially at hub heights beyond 140 m.

The calculated protection areas are illustrated in the figure below. The Effelsberg radio telescope is situated in the centre of the figure, the locations of the planned turbines are marked in blue.

In the areas coloured red, the operation of a single turbine of the types measured would cause interference to the radio telescope. In the white areas, it would be possible to operate a single wind turbine and in the green area it would be possible to operate six of the measured wind turbines without causing interference to the telescope.

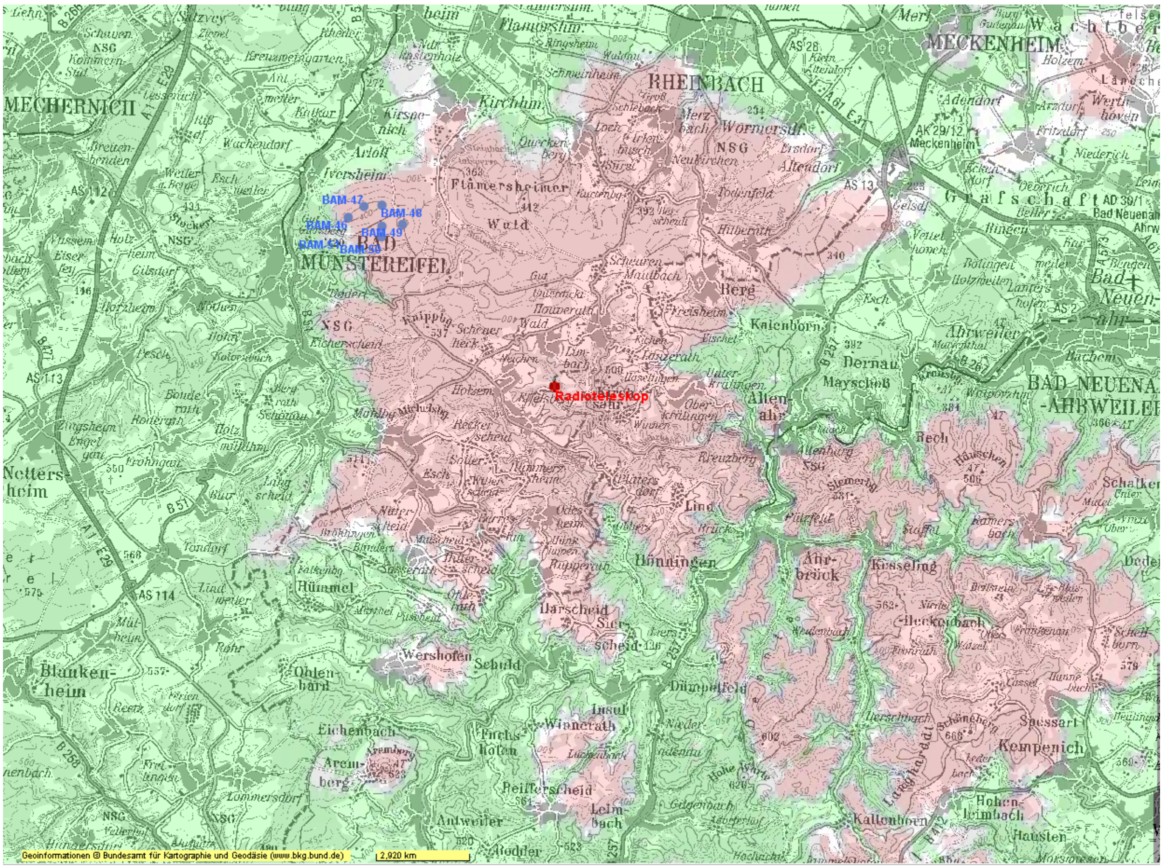

Figure 20: Protection area around the Radio Telescope Effelsberg for the measured wind turbines

A2.13 CONCLUSION

The measurements yielded the following main findings:

- The radiation levels of the measured wind turbines would be well below the limits specified in DIN EN 55011 (up to 1 GHz). They were 25 dB to 31 dB below the limits;

- The protection areas towards wind turbines necessary to ensure interference-free radio astronomical measurements are much lower than assumed in a worst case scenario based on exploiting the EMC limits in full;
- Despite the low radiation levels measured, the wind turbines situated at the planned six sites would still cause interference to continuum observation measurements carried out by the telescope. If more than six wind turbines were to be installed within a 20 km radius, the interference power would increase and would require larger protection areas than set out in Section A2.11.

Special attention is drawn to the fact that, especially at 1413 MHz, measurements were only carried out on three wind turbines, although these models are currently the ones most commonly used. The extremely low radiation levels measured at 1413 MHz are not legally binding for manufacturers and operators of wind turbines and should not be assumed to apply to all installed turbines. Yet the measurements do show that interference levels well below the limits in EN 55011 [20] are achievable with state-of-the-art technology and without additional efforts to suppress spurious radiation.

At a distance of 200 m, the received interference power levels of the measured wind turbines were far below the noise levels from other sources (including MMN) that have to be tolerated by telescope operators even today. However, most of the natural and background noise contributions are approximately white and can be effectively reduced by long integration times. As such, the present study constitutes a worst-case scenario based on the assumption that, owing to its spectral characteristics, the interference from wind turbines cannot be eliminated during measurements whereas other noise levels can be.

ANNEX 3: A METHODOLOGY FOR RAS – WIND TURBINE COMPATIBILITY STUDIES

A3.1 INTRODUCTION

Radio astronomical stations and wind power generators are large engineering structures and expensive to build and operate. Impairments of their operation lead inevitably to a great loss of either scientific output in the case of radio astronomical stations that are publicly funded or to loss of revenue for the often private operators of wind turbines. Compatibility studies are therefore already imperative in the early planning stages of wind power deployment so that costly mistakes may be avoided.

The specific interference vulnerability of the RAS has been described in Recommendation ITU-R SM.1542-0 [19] and a methodology to calculate limits on received interference for RAS stations is outlined in Recommendation ITU-R RA.769-2 [15]. The emissions from wind turbine electronics are mainly attenuated by path propagation and here Recommendation ITU-R P.452-16 [3] provides the methodology for calculation of the attenuation. We implemented the path propagation method of this recommendation in a Python software package, “pycraf”. As Recommendation ITU P.452 needs topographic information, pycraf can automatically query terrain heights from data sets such as the Space Shuttle Radar Mission (SRTM; [2]) or Light Detection and Ranging (LIDAR) campaigns. Combined with the threshold levels defined in Recommendation RA.769 [15] and an estimate of the emitted power, the user can assess the impact of a wind turbine of a given height on a proposed location.

A3.2 TECHNICAL PARAMETERS

A3.2.1 Emissions from Wind Turbines

In terms of electromagnetic interference (EMI) regulations, wind turbines count as industrial devices (Group 1, Class A), which are required to conform to the EN 550011 (also known as CISPR-11) standard [20]: the electrical field strength measured at a distance of 30 m with a quasi-peak (QP) detector having a bandwidth of 120 kHz must not exceed 30 dBμV/m below 230 MHz or 37 dBμV/m between 230 MHz and 1 GHz. (Here the CISPR-11 specification is used for the appropriate bands C and D, 30 MHz−1000 MHz.)

In addition to their main power generators and conversion equipment the wind power generators may also use computerised and networked control and telemetry equipment that may be covered by e.g. the recommendations provided in Recommendation ITU-R SM.329-12 [16].

CISPR-11 limits are not explicitly specified for frequencies above 1 GHz. Furthermore, for other applications above 1 GHz the CISPR committee typically uses a different bandwidth (1 MHz) for the measurement channel. Reference bandwidths of 100 kHz for frequencies above 30 MHz and below 1000 MHz and 1 MHz for frequencies above 1000 MHz are also recommended in Chapter 4.1 of Recommendation ITU-R SM.329-12.

We assume here, that the emissions are limited to the CISPR-11 levels but different measurement-based, emission limits may also be used if they are available. The CISPR-11 electrical field limits are defined for a certain measurement bandwidth also specified by CISPR-11. In order to compare them with RAS thresholds from Recommendation ITU-R RA.769-2, one will have to calculate the power that is going to be emitted over the appropriate RAS bandwidth. RAS interference limits are defined as averages, while CISPR-11 limits below 1 GHz refer to quasi-peak detections, where the envelope of the received power as a function of time from a chosen detector band is fed to an additional post-detection integrator that has several time constants : a $t_{\mathrm{c}} = 1\ \mathrm{ms}$ rise time of the output for any input signal that is greater than the current output level, and a $t_{\mathrm{d}} = 550\ \mathrm{ms}$ decay time when the input level is below the output level. This results in a saw-tooth output for time variable inputs which is further smoothed with a ‘meter’ time constant $t_m = 100\ \mathrm{ms}$ [4].

CISPR-11 specifies only QP limits for the relevant bands C and D, corresponding to the peak power for continuous or high repetition rate ($t_{\mathrm{rep}} < t_{\mathrm{d}}$) which can be about 3 dB higher than the average power, but tend to reflect the averaged power for low duty cycle ($t_{\mathrm{rep}} > t_{\mathrm{d}}$) signals [5]. As most interference emissions are by nature highly variable in time and frequency, it is assumed that the CISPR-11 QP limits may also provide a worst-case upper limit for the long (2000 s) typical time averages specified for radio astronomy protection. The CISPR-11 limits take neither the temporal nor the spectral signature of possible EMI emissions into account.

Furthermore, it is not known whether the electrical and electronic equipment in the wind turbine hub and foot produces a flat spectrum or only a limited number of relatively narrow spectral lines, such as harmonics from oscillators in digital equipment.

Emissions from such ITE equipment may also be limited in accordance to the treatment of category Z for industrial equipment in Table 6 of Recommendation ITU-R SM.329-12 [16].

Table 12: Category Z limits for ITE equipment with radio transmission functionality (source: Recommendation ITU-R SM.329-12)

Frequency [MHz]	Emax [dB(µV/m)]	Distance of measurement [m]	Corresponding e.i.r.p. [dBm]
20−230	40(1)	10	−49
230−1000	47(1)	10	−42
1000−3000	76(2)	3	−23
3000−6000	80(2)	3	−19
Quasi-peak limit Peak limit			

Note that these limits are less stringent for frequencies above 1 GHz than those adopted in the subsequent study and particular care and attention is required for the coordination with RAS with wind power generators that have industrial category Z equipment installed in the nacelle.

A3.2.2 RAS station parameters

Although being only a receiving (passive) service, radio astronomy service (RAS) is recognised as a full radio service according to Article 4.6 of the Radio Regulations (RR) [22]. A number of frequency bands sampling the range between 13 MHz and 270 GHz has been allocated to RAS (RR. Vol. I, Chapter II) and is used by RAS stations, depending on their location, technical instrumentation and research focus. RR FN 5.149 lists frequency bands for which '...administrations are urged to take all practicable steps to protect the radio astronomy service from harmful interference. Emissions from spaceborne or airborne stations can be particularly serious sources of interference to the radio astronomy service (see Nos. 4.5 and 4.6 and Article 29).' In addition, there are frequency bands which are entitled to an even stricter protection by RR. FN 5.340 where '...All emissions are prohibited in the following bands: [List]...'.

Commonly used protection criteria for RAS are listed in Recommendation ITU-R RA.769-2 [15] and e.g. Table 8 of ITU-R SM.329-12. Both, FN 5.149 and Recommendation ITU-R RA.769-2 emphasise the vulnerability of RAS to sources of interference that are high above the ground level, as it would be the case with wind power generators in the vicinity of RAS stations, where both wind power generators and RAS antenna have typically no shielding by local clutter.

Table 13: Limits for emissions and received radio powers in selected bands that are allocated to RAS

v RAS centre frequency [MHz]	ΔvRAS [MHz]	PRA.769 Received in-band power limit [dBW]	Permitted field strength (CISPR-11) [dB(μV/m)]	Pem Corresponding e.i.r.p in RAS bandwidth [dBW]	MCL [dB]
325.3	6.6	-201	37	-60	141
408.05	3.9	-203	37	-62	141
611	6.0	-202	37	-60	142
1414	27	-205	37	-54	151
1665	10	-207	37	-58	149

Table 13 gives a comparison of emission and reception limits pertaining to UHF and L-Band frequencies. Here a reference bandwidth of $\Delta\nu_{C11} = 1\,\mathrm{MHz}$ for the emissions is used, and it is assumed that the full emission level is present over the RAS bandwidth $\Delta\nu_{RAS}$. Then the e.i.r.p. in the RAS bandwidth is calculated as

$$\mathrm{EIRP_{RAS}[dB_W]} = E_{\mathrm{C11}}\left[\mathrm{dB}_{\frac{\mu V}{m}}\right] + 20\log_{10}(d_0[\mathrm{m}]) + 10\log_{10}\left(\frac{\Delta\nu_{\mathrm{RAS}}}{\Delta\nu_{\mathrm{C11}}}\right) - 134.8 \quad (18)$$

A3.2.3 Mitigations and minimum coupling loss

The main attenuation mechanism is the path propagation loss between the emitter and the receiver, but the antenna gains will also play a role for the coupling loss. A generic omnidirectional 0 dBi gain for both patterns is assumed. The actual gain under all circumstances in the direction of the wind turbines would have to be considered when their locations for potential implementation are known, which is usually not done for practical reasons.

On the one hand, wind turbines are not antennas by design and to our knowledge no studies exist that examine the effective pattern of radio emission emanating from a wind turbine when radio frequency currents are excited in the structure. In the absence of specific information, a simplified scenario where the source of emissions is located is used at the height of the nacelle (hub) of the wind power generator.

For the RAS station, on the other hand, the antenna pattern can be measured and modelled, and Recommendation ITU-R RA.1631 [18] provides a simplified description of a “standard antenna” for compatibility studies. Recommendation ITU-R SM.1542-0 [19] however stresses that radio astronomical antennas are already designed for optimal main beam versus side lobe reception.

The RAS antenna usually points towards an astronomical object of interest located anywhere on the visible sky, being in motion w.r.t. the horizontal coordinate system, while wind turbines are located close to the local horizon as seen from the telescope. A wind turbine is therefore more or less equally likely positioned anywhere in the antenna pattern, resulting in an average receiving gain of about 0 dBi. There are however conceivable situations, where a radio telescope observes a source close to the horizon and in a flat countryside it could even happen that the wind turbine is within the main-beam direction. Then, the full forward antenna gain (up to ≈90 dBi, depending on dish size and frequency) would even allow the detection of thermal emission from the rotor blades at ambient temperature. Clearly such a situation must be avoided by either placing wind turbine only in locations where they are outside the line of sight, or, alternatively, the operations of the RAS station will have to be restricted to higher elevation angles, leading to a loss of available sky for its operations.

Recommendation ITU-R SM.1542-0 outlines that there are no operational mitigations from the RAS side, at least none that will not have significant restrictions of the operation of the RAS station.

The wind power installation may however by design operate with smaller than the permitted emission levels, or by restricting interference to a fraction of the allocated RAS band. Mitigating factors A_{m} may therefore be derived on a case by case basis as the result of appropriate measurements for the type of wind turbine that is planned for the site under consideration. Meaningful measurements are those that provide representative information about the frequency and time averaged emissions of the wind turbine at the height of the hub/nacelle. The averaging should be matched to the allocated RAS band width and an integration time of 2000 s which is typical for the specification of RAS interference limits. The mitigation factor is then simply given by $A_{\mathrm{m}}[\mathrm{dB}] = 10\log_{10}(\frac{P_{\mathrm{meas}}}{P_{\mathrm{em}}})$, which is also true for the case of possible larger emissions from ITE equipment of e.g. category Z. One will set $A_{\mathrm{m}} = 0\ \mathrm{dB}$ for the generic case, i.e., in the absence of evidence for mitigations based on e.g. measured spectrograms.

If the terrain-dependent path attenuation to the RAS station does not vary greatly across the proposed site, then one expects an additive increase of the interference in those cases where a number N_{WT} of similar wind turbine are to be deployed at a common location (wind park).

Hence the required minimum coupling loss for protection (MCL) is given by

$$\mathrm{MCL}[\mathrm{dB}] = P_{\mathrm{em}}[\mathrm{dB_W}] + A_{\mathrm{m}}[\mathrm{dB}] + 10\log_{10}(N_{\mathrm{WT}}) - P_{\mathrm{RA.769}}[\mathrm{dB_W}] \quad (19)$$

Table 13 lists the MCL for selected RAS allocations in UHF and L-Band.

A3.2.4 Path propagation loss

The calculation of path propagation losses between two terminals is based on the method described in Recommendation ITU-R P.452-16 [3]. It accounts for a variety of propagation/attenuation mechanisms such as:

- Line-of-sight (free-space) loss including correction terms for multi-path and focussing effects;
- Diffraction (at terrain features);
- Tropospheric scatter;
- Anomalous propagation (ducting, reflection from elevated atmospheric layers).

While for many other compatibility studies, the effect of clutter has to be incorporated into the calculation, modern wind turbine have heights that significantly exceed typical clutter heights. We assume that the hub (nacelle) of the wind turbine will be the most important source of radio interference whereas the base and lower parts of the support structure may also radiate, but their radiation will be more strongly absorbed by local clutter and topography. The receiver terminal (the radio telescope) is also higher than surrounding clutter to avoid picking up thermal radiation from objects in the vicinity. However clutter between RAS site and WT location may have an impact that would have to be considered on a case by case basis.

Zero clutter loss for all following calculations is assumed. The scattering at rain drops (so called hydrometeor scattering) can sometimes play a role, but this effect will also be neglected here.

Note, that attenuation by the atmosphere, caused by the oxygen and water content in the lower layers of the atmosphere, is accounted for in the line-of-sight and diffraction terms of the Recommendation ITU-R P.452-16 propagation algorithm, based on the methods described in Recommendation ITU-R P.676 [17].

The path loss resulting from the Recommendation ITU-R P.452 algorithm has to be understood in statistical terms: the loss value $L(p)$ returned for a given p means that only with a probability of p will the true path loss be higher than $L(p)$. The function $L(p)$ is in fact the inverse of the cumulative distribution function of the loss values. For radio astronomical observations it needs to be ensured that the RAS thresholds are not exceeded for most of the time, so that only a small fraction of data may be lost. Therefore, $p = 2\%$ for all subsequent calculations is used. This choice of percentage is typical for the regulatory constraints by the ITU-R on interference probabilities from other services that might affect RAS.

A Python implementation of Recommendation ITU-R P.452-16 exists, in the form of the Python library "pycraf", and is available as open-source software (GPL-v3) on the Python package distribution server PyPI (Python

Package Index) [10]. The software repository is hosted on GitHub [11], along with detailed documentation and tutorials [12]. For details one may refer to the pycraf documentation and Recommendation ITU-R P.452.

A3.3 SINGLE INTERFERER SCENARIO GENERIC RESULTS

An initial consideration of the so-called generic case, in which terrain heights are neglected ("Flat Earth" scenario) can however be quite illustrative. These generic results already provide a first estimate of the separation distances that may perhaps be required, and can be a useful guideline for all involved parties: radio astronomers, wind turbine manufacturers/operators, and local planning authorities.

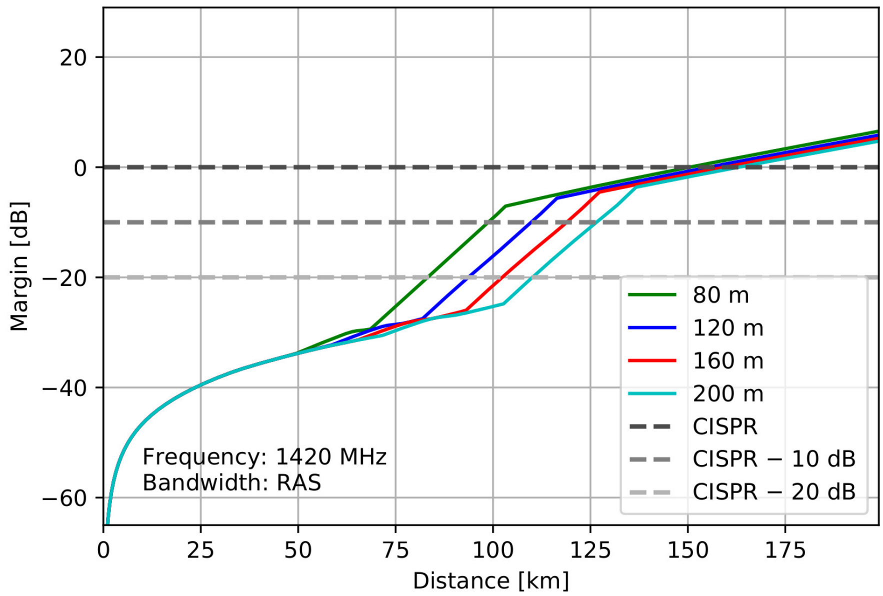

Figure 21: Generic compatibility margins assuming emissions on CISPR-11 with possible mitigations levels as a function of distance for $\nu = 1420\ \mathrm{MHz}$ and differing hub heights

Subtracting the MCL from the path loss values yields the (link-)margin:

$$\mathrm{Margin[dB]} = L(p = 2\%)\mathrm{[dB]} - \mathrm{MCL[dB]} \tag{20}$$

If it is zero, then a wind turbine would just be compatible with the RAS power limits at that location. Negative margins indicate a situation where compatibility is compromised. The above figure shows the results of generic example calculations for the very important 1420 MHz RAS band and for varying hub heights.

It is noted that for the generic scenario, the $\mathrm{Margin} = 0\ \mathrm{dB}$ distance is beyond the visual horizon even in cases of low hub heights and emissions that are 20 dB below the levels allowed by CISPR-11. Wind turbine turbines could not be closer to the RAS station than 75 km in the best generic case. This serves to illustrate the gravity of the problem for all cases where the terrain will not provide adequate shielding of emissions. The necessary separation distances would be even larger for emissions that are higher than those permitted by CISPR-11, e.g. from category 'Z' ITE equipment, or other types of radio equipment such as radar or fixed link installations.

A3.4 CASE STUDY USING TOPOGRAPHY

The generic analysis discussed in the previous section can only provide a rough estimate of necessary separation distances, because in reality the radio telescopes are not situated in a completely flat environment. Therefore, the topography around a specific site must be taken into account, and that can have a substantial influence on the path attenuation, especially when one considers the diffraction on terrain obstacles.

An example of terrain-dependent calculations for the Effelsberg 100 m radio telescope is provided. The 100-m dish is located at the northern edge of the Eifel mountains in Germany. As for the generic case, the total path propagation loss is calculated according to Recommendation ITU-R P.452-16 [3] employing the pycraf software package. With pycraf one can make use of terrain height data as e.g. provided by the SRTM Space Shuttle Mission [2]. We discovered by comparing SRTM with other topography data sets that the SRTM data for the chosen RAS site has larger than usual height errors. In this particular example, Light Detection and Ranging (LIDAR) is therefore used based topography data, which has been provided by the German regional ('Länder') administrations for North-Rhine-Westphalia [23] and Rhineland-Palatinate [13].

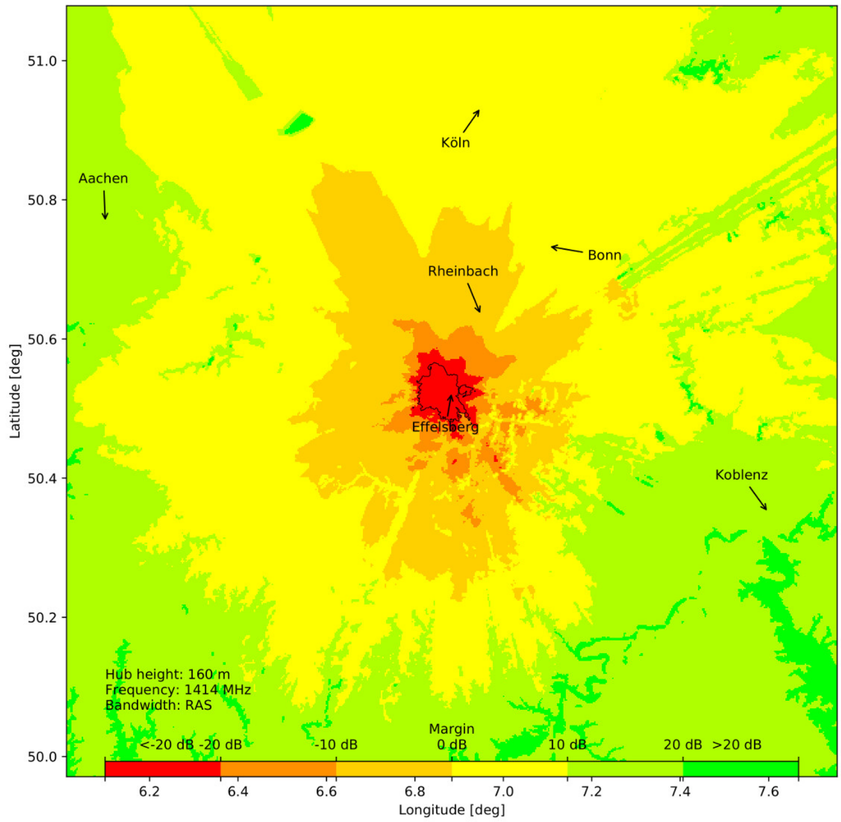

Figure 22: Margins for wind turbine with emissions up to the CISPR-11 limit at $\nu = 1420$ MHz and a hub height of 160 m. The critical areas below 0 dB margin have been coloured in red and orange, while positive margins are indicated with yellow and green. The (radio-wave) horizon (as seen from the telescope centre) is indicated with a black contour

An example map of margins for ν=1414 MHz using the path attenuation according to Recommendation ITU-R P. 452-16 [3] is provided as implemented in pycraf in Figure 22. As expected, the $\mathrm{Margin} < 0$ dB zone is now significantly reduced when compared to the generic case. One notes however that compatibility with RAS operations will still be compromised beyond the visual horizon − even for additional mitigations of 20 dB.

A3.5 SUMMARY

A method to calculate the potential level of interference that a wind turbine farm could produce in a radio astronomical receiving system is based on three basic steps:

- estimating the amount of power that could be produced in the wind turbine (electric and electronic devices in the hub);
- determining the attenuation between wind turbine and RAS receiver, i.e., the path propagation loss according to Recommendation ITU-R P.452-16 [3];
- comparing the consequently received power with the permitted RAS power limits given in Recommendation ITU-R RA.769-2 [15].

For the first step, measurements of the emitted power would be needed. This will vary for different types of wind turbine, and a significant effort is required to perform these measurements. If such information is lacking one has to use the maximally permitted power that an industrial device may emit, as given in EN550011 (CISPR-11)[20] .

The generic separation distances between a single wind turbine and the RAS antenna are of the order of 150 km if the wind turbine fully exploits the CISPR-11 limits and local terrain effects are negligible (spherical earth approximation). Measurements of real installations indicate that the true emitted power is often up to twenty or more Decibels below CISPR-11 levels, in which case the generic separation distances shrink to values between about 75 and 125 km, depending on the hub height of the WT. Generic estimates are however only useful for an initial evaluation of the possible severity of the general compatibility problem.

Detailed investigations considering the actual emissions of the proposed type of installation and the effect of the topography along the path between RAS antenna and wind turbine must be undertaken for each individual case. The diffraction on the hill and mountain tops along the propagation paths to a wind turbine farm may substantially attenuate the signal from there. As a result, hence the required separation distances will become much smaller, very often of the order of 20 to 30 km, depending on the azimuthal direction (because the terrain is not isotropic with respect to the RAS station location), height of the wind turbine and other obstacles if any. In relevant cases RAS antenna gain could also be considered.

ANNEX 4: MEASUREMENT OF THE RADAR CROSS SECTION OF A WIND TURBINE

A4.1 INTRODUCTION

In September 2019 the radiocommunications Agency of the Netherlands performed a radar cross section (RCS) measurement on an experimental wind turbine in Nieuw Buinen, the Netherlands. The wind turbine is constructed with very low EMC emissions in mind and is the first one of a series of 45 planned for the wind farm 'Drentse Monden en Oostermoer'. Since the wind farm is located in the vicinity of the core of the highly sensitive LOFAR radio astronomy telescope, there is a substantial risk that the electronic circuits inside and around the wind turbines will cause interference to LOFAR. Therefore, the initial wind turbine is acting as a test vehicle for performing EMC emission tests using LOFAR. Besides emissions from the wind turbine itself, the whole installation, the 134 m high tower, the nacelle and the 131 m diameter rotating blades, represents a large reflecting area and therefore may reflect emissions from ground-based sources in the neighbourhood (e.g. PV installations), which formerly were below LOFAR's observation horizon. For this reason, RCS measurement of the wind turbine is done, at frequencies used by LOFAR, to provide valuable input data to the interference model of the environment.

A4.2 MATERIALS AND METHOD

To perform an RCS measurement, one has to send a known amount of RF energy towards a reflecting object, to receive the returning part and to compare the difference. In order to obtain a functional and accurate measurement setup, several things should be taken into account. Since the reflected energy is mostly many orders of magnitude smaller than the transmitted energy, the measurement equipment should be capable providing a large dynamic range. Besides the transmitter output power and the receiver sensitivity, the isolation between transmitter and receiver is of major importance. Secondly, the measurement equipment should be capable of distinguishing the right echo, as the object-of-interest might be one amongst many others in a certain direction. Hence, the reflected signal should be observed in the time domain (i.e. range) with sufficient resolution. Taking the above into account, a network analyser[1] happens to be the optimal instrument for this type of measurement, because of its capability to perform accurate transmission measurement over a very large dynamic range and to visualize the measurement data in the time domain (by performing and inverse Fourier transformation). At each port of the network analyser two identical log-periodic antennas[2] are connected, covering LOFAR's operational frequency range. Prior to measurement, the equipment, including the cabling, has been calibrated, shifting the reference plane to be at both the antenna connectors.

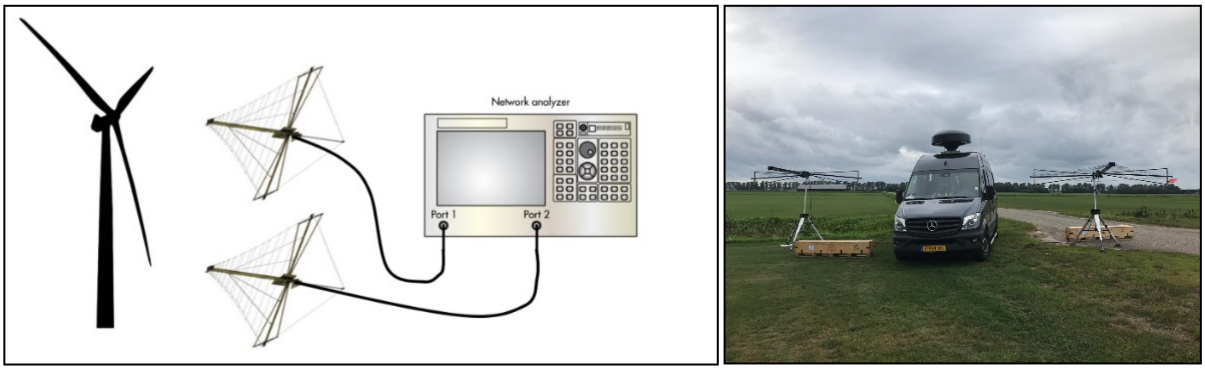

Figure 23: Measurement setup schematic view and actual installation

To obtain sufficient isolation between the antennas, the measurement vehicle has been positioned in between. Both antennas are pointed towards the wind turbine at a distance (R) of approx. 1.7 km away from the measurement setup. During the measurement, the wind direction and the line-of-sight toward the wind turbine nearly matched, causing the RCS to be determined about perpendicular to the rotating plane of the blades. This constellation is considered to yield the highest possible reflection from the rotating part of the wind turbine.

---

[1] Agilent Technologies E5072A network analyser

[2] Alaris LPDA-A0097 wideband wire LPDA antenna, mounted at 2 m height above ground level

Because of maintenance work at the wind turbine the rotating speed of the blades was very low. This could influence the orientation of the blades, which might be different from operational conditions.

The measurements have been done at two frequencies (f), 57 MHz and 310 MHz[3], at which the gain of the antennas (Ga) is 1 dB and 6 dB respectively. Before selecting a measurement frequency it is important to find an 'empty' part of the spectrum, free of extraneous signals (e.g. broadcast)[4].Although the transmitter power applied is equal to 20 dBm, it is basically irrelevant knowing that the network analyser instantly shows the ratio of the transmitted and received powers (P_r/P_t). The analyser uses a frequency chirp as a form of pulse compression. The RCS cannot be measured directly, but knowing the parameters noted above, the RCS can be calculated using the following expression:

$$RCS = \frac{power\ reflected\ towards\ source\ /\ unit\ solid\ angle}{incident\ power\ density\ at\ the\ object\ /\ 4\pi} \tag{21}$$

$$RCS = {P_r}/{P_t} * \frac{(4\pi)^3 * R^4 * f^2}{2 * G_a * c^2} \tag{22}$$

Where:

- c is the velocity of light in vacuum;
- G_a= overall gain of the two antennas;
- F= frequency in MHz;
- R= distance in m.

A4.3 MEASUREMENT RESULTS

The below figure show the results of the measurement at 57 MHz and 310 MHz. The horizontal axis shows the time (2 µs/div), which represents the distance towards reflecting objects[5]. On the vertical axis the ratio between received and transmitted power is shown (10 dB/div).

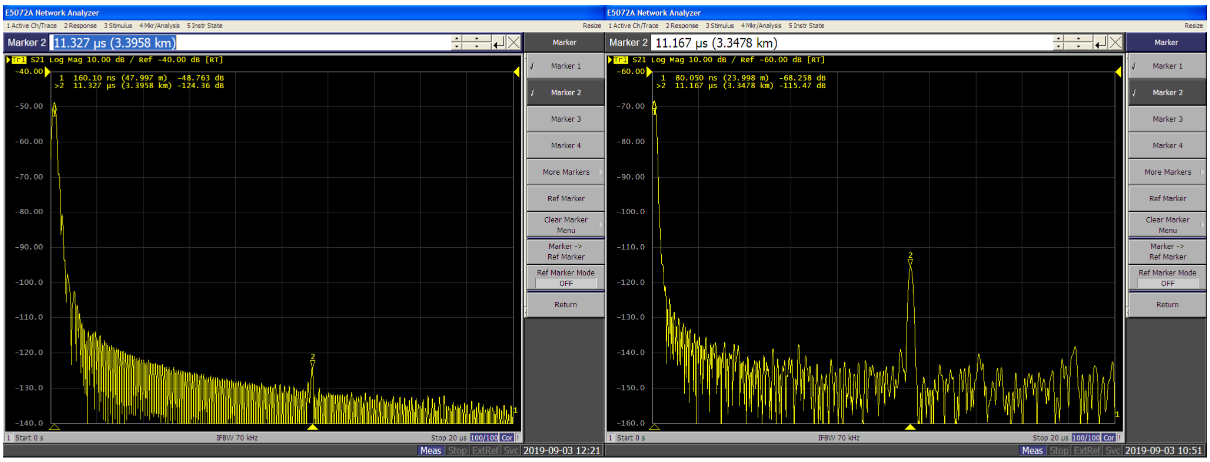

Figure 24: Echo plots of the wind turbine at 57 MHz (left) and 310 MHz (right).

At the far left side of the plots (t = 0) marker 1 is showing the isolation between the antennas, which equals -48 dB @ 57 MHz and -68 dB @ 310 MHz. Marker 2 shows the reflected signal from the wind turbine at 11 µs,

---

[3] The frequencies of measurement were chosen such not to interfere with Lofar's measurement campaign.

[4] The necessary measurement bandwidth relates to the required range resolution. In this case a bandwidth of 10 MHz was used.

[5] The reading of the network analyser shows twice the length of the path travelled by the measurement signal.

which has a maximum value of -124 dB @ 57 MHz and -115 dB @ 310 MHz. The actual value of the reflected signal varies substantially, due the rotation of the blades. From these results the RCS can be calculated using the expression above, which yields a maximum RCS of 22 dBm2 (160 m^2) @ 57 MHz and 35 dBm2 (3200 m^2) @ 310 MHz.

A4.4 REMARKS AND LIMITATIONS

- RCS is only valid in the far field[6], this measurement is performed at 1.7 km distance on an object of 150 m height. It can be argued that therefore the measurement of the reflected signal is inaccurate, however the dispersion of the received pulse can be used to assess the severity of this condition. A distance of 1.7 km showed a good compromise between accuracy and sensitivity of the setup.

  Considering that the wind turbine is in fact a large dimension re-radiator of signals, one could argue that, within the range of frequencies used by LOFAR, the distance at which the measurement takes place is smaller than the electromagnetic far-field distance. Unfortunately, a measurement distance equal or larger than the far-field distance cannot be met, because an even larger dynamic range of the measurement setup would be required. Besides, it would be much harder to distinguish the target in the time domain. Hence, the applied measurement location is a compromise between the electromagnetic field distance and the dynamic range of the measurement setup.
- The log periodic antennas are placed low above ground so segmentation of the main lobe will occur for the lower frequencies. This is not problematic since two identical antennas are used but it has to be assumed that the whole construction reflects in a similar matter. Indications are that this is not the case for the lowest frequencies.

---

6 For the boundary between the electromagnetic near-field and far-field a distance equal to $2D^2/\lambda$ is often applied

ANNEX 5: LIST OF REFERENCES

[1] ECC Report 260: “Description of methodologies to estimate the technical impact of Wind Turbines on Fixed Radio Links”, approved January 2017

[2] Mike J. Wills: “SRTMPathProfile software” www.mike-wills.com/software.html

[3] Recommendation ITU-R P.452-16: “Prediction procedure for the evaluation of interference between stations on the surface of the Earth at frequencies above about 0.1 GHz”

[4] B. Winkel and A. Jessner: “Spectrum management and compatibility studies with Python,” Advances in Radio Science, vol. 16, pp. 177-194, 9 2018”

[5] B. Winkel and A. Jessner: “Compatibility Between Wind Turbines and the Radio Astronomy Service,” arXiv e-prints, p. arXiv:1812.04731, 12 2018. etc.”

[6] T. G. Farr, P. A. Rosen, E. Caro, R. Crippen, R. Duren, S. Hensley, M. Kobrick, M. Paller, E. Rodriguez, L. Roth, D. Seal, S. Shaffer, J. Shimada, J. Umland, M. Werner, M. Oskin, D. Burbank and D. Alsdorf, “The Shuttle Radar Topography Mission:” Reviews of Geophysics, vol. 45, 2007”

[7] International Special Committee on Radio Interference (CISPR):”Industrial, scientific and medical (ISM) radio-frequency equipment -- Electromagnetic disturbance characteristics -- Limits and methods of measurement”, Geneva, 2015.

[8] F. Krug, S. Braun and P. Russer: “A novel quasi-peak-detector for time-domain EMI-measurements,” Advances in Radio Science, vol. 2, pp. 27-32, 5 2004.

[9] D. Ristau and D. Hansen: “Modulation impact on quasi-peak detector response,” in IEEE 1997, EMC, Austin Style. IEEE 1997 International Symposium on Electromagnetic Compatibility. Symposium Record (Cat. No.97CH36113), 1997

[10] B. Winkel, “Python Package Index (PyPI): pycraf” https://pypi.org/project/pycraf/.

[11] B. Winkel, “pycraf GitHub repository,” https://github.com/bwinkel/pycraf.

[12] B. Winkel, “pycraf online documentation/user manual,” https://bwinkel.github.io/pycraf/latest/.

[13] GeoBasis-DE / LVermGeoRP, “Data license Germany - attribution - Version 2.0,” 2018 https://www.govdata.de/dl-de/by-2-0

[14] A. Jessner: “Industrial interference and radio astronomy”, Adv. Radio Sci., 11, 1–8, 2013, www.adv-radio-sci.net/11/1/2013/

[15] Recommendation ITU-R RA.769-2: “Protection criteria used for radio astronomical measurements”

[16] Recommendation ITU-R SM.329-12: “Unwanted emissions in the spurious domain”

[17] Recommendation ITU-R P.676: “Attenuation by atmospheric gases and related effects”

[18] Recommendation ITU-R RA.1631: “Reference radio astronomy antenna pattern to be used for compatibility analyses between non-GSO systems and radio astronomy service stations based on the epfd concept”

[19] Recommendation ITU-R SM.1542-0: “The protection of passive services from unwanted emissions “

[20] IEC EN 55011 CISPR 11: “Industrial, scientific and medical equipment Radio-frequency disturbance characteristics – Limits and methods of measurement”

[21] IEC EN 61000-6-3: “Generic standards - Emission standard for residential, commercial and light-industrial environments”

[22] ITU Radio Regulations Edition of 2016

[23] Land NRW, “Data license Germany - attribution - Version 2.0,” 2018 https://www.opengeodata.nrw.de/produkte/geobasis/hm/dgm1_xyz/